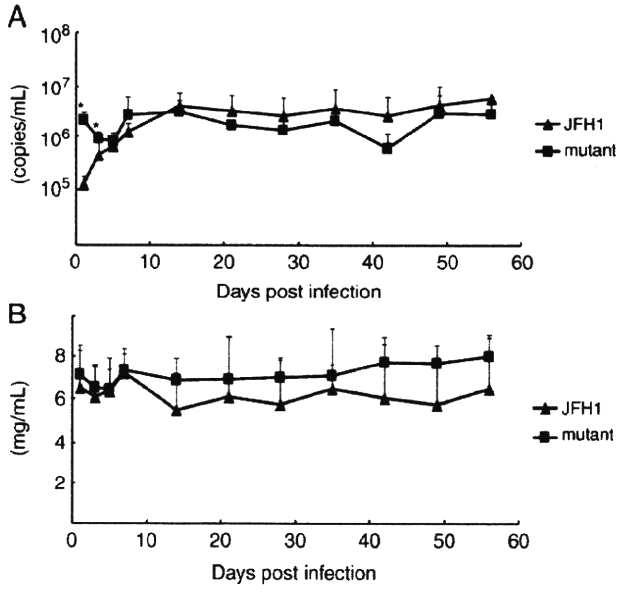

Fig. 6. In vivo analysis of cytopathic JFH1 mutants using human hepatocyte chimeric mice. A. Serial changes in HCV RNA in the sera of mice inoculated with the culture media from JFH1 mutants. The data shows the average of 2 mice for JFH1, and 3 mice for the mutant. Asterisks indicate p-values of less than 0.05 as compared with JFH1. B. Levels of human albumin in the sera of mice inoculated with the culture media from JFH1 mutants.

inoculated with the cytopathic mutant virus showed conservation of the mutations in codons 2441, 2938 and 2985. However, on days 21 and later, the mutation at codon 2985 had reverted to the wild type JFH1 sequence in all the mutant-injected mice and the mutation at codon 2938 had reverted to the wild type JFH1 sequence in two of the three mice. The C2441S mutation was more stable in the mutant-injected mice, but one mouse had lost it at day 56 (Fig. 8).

Discussion

In this study, we investigated the significance of genetic mutations in plaque-purified, cytopathic HCV-JFH1 subclones. Genetically engineered JFH1-mutants encoding C2441S, P2938S, and R2985P led to much more cell death than the wild type JFH1, and also produced significantly higher amounts of core antigen in the culture medium and inside the cells than the parental JFH1 clone. In the single-cycle production assay, which exploited a receptor-deficient Huh7 cell line, the three JFH1-mutants, JFH1-C2441S, P2938S, and R2985P produced significantly more core antigen in the culture medium and expressed equivalently higher amounts of viral genomic RNA in the cells. These data suggest that the three mutations in NS5A and NS5B (C2441S, P2938S, and R2985P) are associated directly with enhanced intracellular replication and resultant virion formation, which correlated with the extent of the cytopathic effects. Interestingly, inoculation of a cytopathogenic mutant, JFH1-C2441S/P2938S/R2985P, into human hepatocyte chimeric mice produced significantly higher plasma HCV RNA concentrations than JFH1 at ~7 days post inoculation. At a later phase of infection, however, the mutations in this mutant HCV reverted partially to the wild type sequences. Taking all things together, it is suggested that in vitro-isolated, genetically modified cytopathic HCV subclones replicate robustly in the acute phase of in vivo infection but are eliminated rapidly and substituted by in vivo adapted clones.

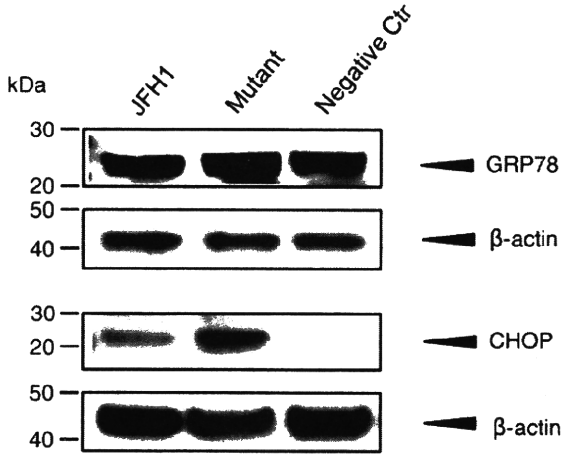

Fig. 7. Expression of ER stress-related proteins in human hepatocytes of chimeric mice infected with JFH1 or the mutant in the early phase. Western-blot analysis of the liver tissues of infected chimeric mice using anti-GRP78 goat monoclonal antibody, anti-GADD153/CHOP rabbit polyclonal antibody and anti-beta-actin. Liver samples were obtained at 5 days after inoculation. The negative control liver samples for this study was from uninfected human hepatocyte chimeric mouse.

Four of the five NS5B mutations appeared independently in several isolated subclones. This made us speculate that these amino acid substitutions may affect the enzymatic activity of RdRp. Mapping of the amino acid substitutions in the RdRp tertiary structure revealed that amino acid 2441 is located on the finger domain, and three amino acids, 2938, 2964, and 2985, are on the outer surface of the thumb domain, which corresponds to the opposite side of the nucleotide tunnel. The other substitutions, 3004 and 3005, are within the domain of the polypeptide linking the polymerase to the membrane anchor (Lesburg et al., 1999). Our preliminary study has shown that the NS5B mutations, P2938S and R2985P, did not affect cell-free enzymatic activities of the RNA polymerase. Thus, it is speculated that these mutations may affect the stability of the HCV replicase complex by altering surface affinity to other nonstructural proteins.

There are several reports on cell culture adaptive mutations in the HCV-JFH1 genome that gave more vigorous and consistent virus expression. Most studies involved prolonged cell culture of HCV-JFH1 or multiple rounds of successive passage onto naïve cells. Zhong et al. detected the E2-G451R mutation after culture for more than 60 days. The mutation led to more efficient production of infectious viral particles than wild type JFH1 (Zhong et al., 2006). Delgrange et al. conducted successive virus infections of naïve cells and identified the E2-N534K mutation that facilitated virus-CD81 attachment, and core-F172C and -P173S that increased secretion of virions (Delgrange et al., 2007). Using a similar method, Russell et al. identified E2-N417S that improved virus–cell attachment, and p7-N765D and NS2-Q1012R that increased virion production (Russell et al., 2008). Kaul et al. reported the NS5A-V2440L mutation, that was close to the C terminus and increased virion production (Kaul et al., 2007). Yi et al. used a chimeric virus of genotype 1a and JFH1 and identified the NS3-Q1251L mutation that resulted in enhanced virus production, possibly through improved interactions between NS2 and NS3 that were required for virion formation (Yi et al., 2002). Han et al. used EGFP-tagged virus and identified the mutually dependent mutations, NS3-M1290K and NS5A-T2438I, which improved virus production synergistically (Han et al., 2009).

Of note is that all of the mutations reported above promoted virion secretion or virus–cell surface interaction and none of them showed any effect on intracellular replication of viral RNA or translation of virus proteins. None of the adaptive mutations reported above overlapped with our cytopathogenic mutations. The mutations that we have identified conferred enhanced virus replication and protein expression in the early/acute stages of infection and subsequently led to massive cell death. Our data and the reports of other groups suggest that the HCV genome evolves to adapt to the host cell environment. Mutations that optimize virus secretion or virus–cell entry may be

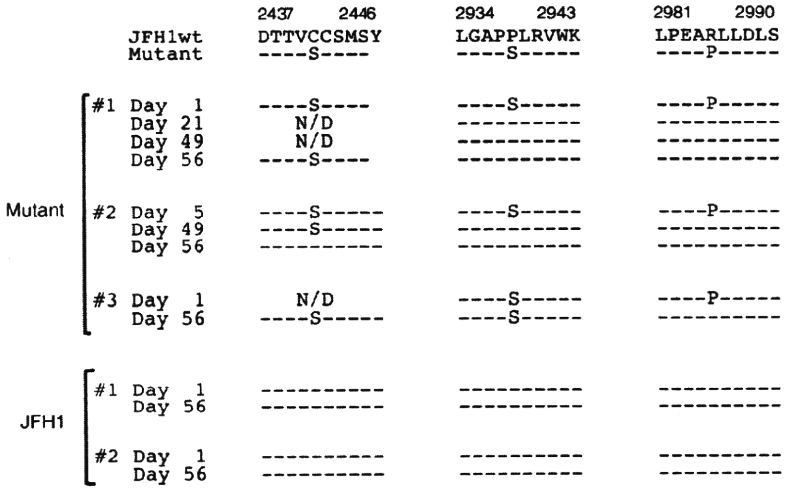

Fig. 8. Nucleotide sequence analysis of virus genomes circulating in the sera of infected mice. We extracted RNA from the sera of mice inoculated with culture media from JFH1 or JFH1-mutants and analyzed the viral sequence at the specified time points. N/D is not detectable. Wt: Wild type.

required for persistent infection in vitro, while those that affect cellular viral RNA replication may possibly promote viral genetic evolution and host cell damage.

The results of in vivo experiments using human hepatocyte chimeric mice were consistent with those of virus cell culture (Figs. 5, 6 and 7). The mutant JFH1 clones showed markedly higher levels of replication than the parental JFH1 in the acute phases. However, the serum HCV titers subsequently leveled out after two weeks of infection, concomitant with reversal of some cytopathic mutations to wild type sequences. Bukh et al. reported that inoculation of the HCV-1b genome into chimpanzee liver resulted in persistent infection, although the mutation reverted rapidly to wild type (Bukh et al., 2002). In this study, the NS5A-C2441S mutation was preserved in 2 of 3 mice, while NS5B-P2938S reverted to the wild type sequences in 2 of 3 mice and NS5B-R2985P reverted to wild type sequences in all 3 mice. These results suggest that the highly adapted JFH1 genome is infectious and viable in vivo, but is not as fit in vitro.

It is not clear why the subgenomic replicons with C2441S, P2938S or R2985P mutations did not show differences in replication levels compared to the wild type JFH1 subgenomic replicon. One may speculate that this discrepancy between the results using full-length HCV genomes and replicons might be the presence or absence of the HCV structural proteins. In addition, three individual substitutions G2964D, H3004Q and S3005N did not enhance viral replication as compared with the parental JFH1 nor did express detectable amounts of core protein. It is speculated that these mutants exist in host cells through co-infection with replication-competent viral clones resulting in enhanced replication.

There is clinical evidence that suggests the pathological outcomes of hepatitis C result from the immune response of the host rather than the direct cytopathic effects of the virus (Cerny and Chisari, 1999). However, several clinical studies have shown that fulminant hepatic failure (FHF, the HCV-JFH1 strain was isolated from such a case) featured massive hepatocyte apoptosis, as characterized by caspase activation and Fas–FasL expression (Leifeld et al., 2006; Mita et al., 2005; Ryo et al., 2000). The ER stress markers, GRP78 and ATF6 are upregulated in HCV-infected liver tissue as the histological grade advances (Shuda et al., 2003). This background and our results in vitro and in vivo suggest that HCV strains with highly infectious and cytopathic gene signatures may replicate aggressively in the acute phase of infection and that certain defects in innate or adaptive immune responses against the virus could lead to severe and persistent liver damage due to cytopathic effects induced directly by HCV. Such mechanisms might explain some rare clinical features of HCV infection, such as fulminant hepatic failure and post-transplantation severe fibrosing cholestatic hepatitis (Delladetsima et al., 1999; Dixon and Crawford, 2007).

In conclusion, we identified three substitutions in cytopathic HCV-JFH1 subclones derived from plaque assay. These substitutions directly enhanced virus replication in the early phases of virus infection in vitro and in vivo. This highly enhanced replication induced ER stress-mediated apoptosis and resulted in cytopathogenicity. Further analyses of cellular effects on HCV replication may elucidate the pathogenesis of HCV infection and may define novel host factors as targets of antiviral chemotherapeutics.

Materials and methods

Cells and cell culture

Huh-7.5.1 cells (Zhong et al., 2005) (kindly provided by Dr Francis V. Chisari) and CD81 deficient Huh7-S29 cells (Russell et al., 2008) (kindly provided by Dr Rodney S. Russell and Dr Robert H. Purcell) were maintained in Dulbecco's modified minimal essential medium (DMEM, Sigma, St. Louis, MO) supplemented with 2 mmol/L L-glutamine and 10% fetal bovine serum at 37 °C under 5.0% CO_2.

Sequence analysis

The cDNA from the isolated JFH1-plaque was amplified from cytopathic virus-infected Huh-7.5.1 cells by RT-PCR and subjected to direct sequencing.

In vitro RNA synthesis and transfection

A plasmid, pJFH1full (Wakita et al., 2005), which encodes full-length HCV-JFH1 sequence, was used. In vitro RNA synthesis and transfection were conducted as previously described (Sekine-Osajima et al., 2008). Briefly, HCV RNA was synthesized from linearized pJFH1 plasmid as template and transfected into Huh-7.5.1 cells by electroporation. The transfected cells were split every 3 to 5 days. The culture media were subsequently transferred onto uninfected Huh-7.5.1 cells and Huh7-S29 cells. The levels of HCV replication and viral protein expression were detected by real-time PCR and western blotting.

Plaque assay

HCV plaque assays were performed as reported previously (Sekine-Osajima et al., 2008). Huh-7.5.1 cells were seeded in collagen-coated 60 mm-diameter plates. After overnight incubation, HCV-infected culture media were serially diluted in a final volume of 2 ml per plate and transferred onto the cell monolayer. After ~5 h of incubation, the inocula were removed and the cell monolayer was overlaid with 8 ml of culture medium containing 0.8% methylcellulose (Sigma). After 7 to 12 days culture, cytopathic plaques were visualized by staining with 0.08% crystal violet solution (Sigma). The levels of cytotoxicity were evaluated by counting the plaques and calculating the titer (plaque-forming unit/ml).

Establishment of mutant JFH1 clones

In order to introduce various mutations into the NS5A and NS5B region of JFH1, plasmid pJFH1 was digested with HindIII and the DNA fragment encompassing nt. 8231 to 9731 was subcloned into the pBluescript II SK+ phagemid vector (Stratagene, La Jolla, CA). Mutations were introduced into the DNA fragment in the subcloning vector by site-directed mutagenesis (Quick-Changell Site-Directed Mutagenesis Kit, Stratagene) to generate the following codon changes: P2938S, G2964D, R2985P, H3004Q and S3005N. Finally, the HindIII–HindIII fragments were subcloned back into the parental plasmid, pJFH1. A PCR fragment (nt. 7421–7839) was subcloned into the pGEM-T Easy plasmid vector (Promega, Madison, WI) and digested with RsrII and BsrGI. Finally, after introducing the codon change C2441S, the RsrII–BsrGI fragment was reinserted into the parental plasmid.

Quantification of HCV core antigen in the culture medium

The culture media from JFH1-RNA transfected Huh-7.5.1 cells and Huh7-S29 cells were collected on the days indicated, passed through a 0.45 μm filter (MILLEX-HA, Millipore, Bedford, MA), and stored at −80 °C. The levels of core antigen in the culture media were measured using a chemiluminescence enzyme immunoassay (CLEIA) according to the manufacturer's protocol (Lumipulse Ortho HCV Antigen, Ortho-Clinical Diagnostics, Tokyo, Japan).

Western blotting

Western blotting was carried out as described previously (Itsui et al., 2009). Briefly, 10 μg of total cell lysate were separated by SDS-PAGE and blotted onto a polyvinylidene fluoride (PVDF) Western Blotting membrane. The membrane was incubated with the primary antibodies followed by a peroxidase-labeled anti IgG antibody, and visualized by chemiluminescence using the ECL Western blotting Analysis System (Amersham Bioscience, Buckinghamshire, UK). The antibodies used were anti-core mouse monoclonal antibody (Abcam, Cambridge, MA), anti-GRP78 goat monoclonal antibody, anti-GADD153/CHOP rabbit polyclonal antibody (Santa Cruz Biotechnology, Santa Cruz, CA), and anti-beta-actin antibody (Sigma).

HCV subgenomic replicon constructs

The HCV subgenomic replicon plasmid, pRep-Feo, was derived from the HCV-N strain, pHCV1bneo-delS (Tanabe et al., 2004; Yokota et al., 2003). The replicon RNA was synthesized from pRep-Feo and transfected into Huh7 cells.

Luciferase reporter assay

Luciferase activity was measured using a 1420 Multilabel Counter (ARVO MX, Perkin Elmer, Waltham, MA) with a Bright-Glo Luciferase Assay System (Promega) (Tasaka et al., 2007). Assays were carried out in triplicate and the results expressed as means ± SD.

MTS assays

To evaluate cell viability, dimethylthiazol carboxymethoxy-phenyl sulfophenyl tetrazolium (MTS) assays were performed using a CellTiter 96 Aqueous One Solution Cell Proliferation Assay kit (Promega), as described previously (Sakamoto et al., 2007).

Real-time RT-PCR analysis

Total cellular RNA was isolated using an RNeasy Mini Kit (QIAGEN, Valencia, CA). Two micro-grams of total cellular RNA were used to generate cDNA from each sample using SuperScript II (Invitrogen) reverse transcriptase. Expression of mRNA was quantified using TaqMan Universal PCR Master Mix (Applied Biosystems) and the ABI 7500 Real-Time PCR System (Applied Biosystems). The primers used were as follows: HCV-JFH1 sense (positions 285 to 307; 5′-GGT-ACTGCCTGATAGGGTGCTT-3′), HCV-JFH1 antisense (positions 349 to 375; 5′-TGGTTTTTCTTTGAGGTTTAGGATTC-3′), GAPDH sense (5′-CCTCCCGCTTCGCTCTCT-3′), and GAPDH antisense (5′-GCTGGCGACG-CAAAAGA-3′).

HCV RNA inoculation into human hepatocyte chimeric mice

Housing, maintenance, and care of the mice used in this study conformed to the requirement for the humane use of animals in scientific research as defined by Animal Care and Use Committee of our institute. The culture media of Huh-7.5.1 cells transfected with parental JFH1 and JFH1 mutants were collected 10 days after transfection and passed through a 0.45 μm filter. The three mutations introduced in NS5A and NS5B were confirmed to conserve by the sequence analysis of virus genome of cell culture supernatants before inoculation. Filtrated culture medium was then pooled and concentrated using Amicon Ultra-15 (100,000 molecular weight cutoff, Millipore). 100 μl of each culture medium was injected intravenously into human hepatocyte chimeric mice (PXB mice, Phenix Bio, Hiroshima, Japan) (Mercer et al., 2001). The rate of liver chimerism of these human hepatocyte chimeric mice was confirmed more than 70% by immunohistochemical analysis. After infection, blood samples were taken serially and levels for HCV RNA and human albumin were quantified using real-time RT-PCR and an enzyme immunoassay, respectively. RNA was extracted from serum samples and subjected to direct sequence determination.

Protein extraction from human hepatocyte chimeric mice and expression of ER stress-related proteins

5 days post inoculation, mice were sacrificed and proteins were extracted from liver samples with complete Lysis-M Reagent Kit (Roche Applied Science, Indianapolis, IN). One Mini Protease Inhibitor Cocktail Tablet was dissolved into 10 ml of Lysis-M Reagent and 500 μl of this fluid was added to 50 μg of each liver sample and homogenized. The lysate was transferred to a microcentrifuge tube and centrifuged at 14,000×*g* for 5 min. The supernatant containing soluble protein was transferred to a new reaction tube and 20 μg of each protein was used for western blotting to detect ER stress-related proteins.

Acknowledgments

We are indebted to Dr. Francis V. Chisari for providing the Huh-7.5.1 cell line and Dr. Rodney S. Russell for receptor-deficient Huh7-S29 cells. This study was supported by grants from Ministry of Education, Culture, Sports, Science and Technology-Japan, the Japan Society for the Promotion of Science, Ministry of Health, Labour and

Welfare-Japan, Japan Health Sciences Foundation, and National Institute of Biomedical Innovation.

References

Alter, M.J., 1997. Epidemiology of hepatitis C. Hepatology 26, 62S–65S.

Bartenschlager, R., Lohmann, V., 2000. Replication of hepatitis C virus. J. Gen. Virol. 81, 1631–1648.

Bukh, J., Pietschmann, T., Lohmann, V., Krieger, N., Faulk, K., Engle, R.E., Govindarajan, S., Shapiro, M., Claire, M.S., Bartenschlager, R., 2002. Mutations that permit efficient replication of hepatitis C virus RNA in Huh-7 cells prevent productive replication in chimpanzees. Proc. Natl. Acad. Sci. U. S. A. 99 (22), 14416–14421.

Cerny, A., Chisari, F.V., 1999. Pathogenesis of chronic hepatitis C: immunological features of hepatic injury and viral persistence. Hepatology 30 (3), 595–601.

Delgrange, D., Pillez, A., Castelain, S., Cocquerel, L., Rouille, Y., Dubuisson, J., Wakita, T., Duverlie, G., Wychowski, C., 2007. Robust production of infectious viral particles in Huh-7 cells by introducing mutations in hepatitis C virus structural proteins. J. Gen. Virol. 88 (Pt 9), 2495–2503.

Delladetsima, J.K., Boletis, J.N., Makris, F., Psichogiou, M., Kostakis, A., Hatzakis, A., 1999. Fibrosing cholestatic hepatitis in renal transplant recipients with hepatitis C virus infection. Liver Transpl. Surg. 5 (4), 294–300.

Dixon, L.R., Crawford, J.M., 2007. Early histologic changes in fibrosing cholestatic hepatitis C. Liver Transpl. 13 (2), 219–226.

Fried, M.W., Shiffman, M.L., Reddy, K.R., Smith, C., Marionos, G., Goncales, F.L., Häussinger, D., Diago, M., Garosi, G., Dhumeaux, D., Craxi, A., Lin, A., Hoffman, J., Yu, J., 2002. Peginterferon alfa-2a plus ribavirin for chronic hepatitis C virus infection. N. Engl. J. Med. 347, 975–982.

Han, Q., Xu, C., Wu, C., Zhu, W., Yang, R., Chen, X., 2009. Compensatory mutations in NS3 and NS5A proteins enhance the virus production capability of hepatitis C reporter virus. Virus Res. 145 (1), 63–73.

Itsui, Y., Sakamoto, N., Kakinuma, S., Nakagawa, M., Sekine-Osajima, Y., Tasaka-Fujita, M., Nishimura-Sakurai, Y., Suda, G., Karakama, Y., Yamamoto, M., Watanabe, T., Ueyama, M., Funaoka, Y., Azuma, S., and Watanabe, M. (2009). Antiviral effects of the interferon-induced protein GBP-1 and its interaction with the hepatitis C virus NS5B protein. Hepatology 50 (6), 1727–1737.

Jordan, R., Wang, L., Graczyk, T.M., Block, T.M., Romano, P.R., 2002. Replication of a cytopathic strain of bovine viral diarrhea virus activates PERK and induces endoplasmic reticulum stress-mediated apoptosis of MDBK cells. J. Virol. 76 (19), 9588–9599.

Kato, N., 2001. Molecular virology of hepatitis C virus. Acta Med. Okayama 55 (3), 133–159.

Kato, T., Date, T., Miyamoto, M., Furusaka, A., Tokushige, K., Mizokami, M., Wakita, T., 2003. Efficient replication of the genotype 2a hepatitis C virus subgenomic replicon. Gastroenterology 125 (6), 1808–1817.

Kaul, A., Woerz, I., Meuleman, P., Leroux-Roels, G., Bartenschlager, R., 2007. Cell culture adaptation of hepatitis C virus and in vivo viability of an adapted variant. J. Virol. 81 (23), 13168–13179.

Koutsoudakis, G., Herrmann, E., Kallis, S., Bartenschlager, R., Pietschmann, T., 2007. The level of CD81 cell surface expression is a key determinant for productive entry of hepatitis C virus into host cells. J. Virol. 81 (2), 588–598.

Leifeld, L., Nattermann, J., Fielenbach, M., Schmitz, V., Sauerbruch, T., Spengler, U., 2006. Intrahepatic activation of caspases in human fulminant hepatic failure. Liver Int. 26 (7), 872–879.

Lesburg, C.A., Cable, M.B., Ferrari, E., Hong, Z., Mannarino, A.F., Weber, P.C., 1999. Crystal structure of the RNA-dependent RNA polymerase from hepatitis C virus reveals a fully encircled active site. Nat. Struct. Biol. 6 (10), 937–943.

Lindenbach, B.D., Evans, M.J., Syder, A.J., Wolk, B., Tellinghuisen, T.L., Liu, C.C., Maruyama, T., Hynes, R.O., Burton, D.R., McKeating, J.A., Rice, C.M., 2005. Complete replication of hepatitis C virus in cell culture. Science 309 (5734), 623–626.

Lohmann, V., Korner, F., Koch, J., Herian, U., Theilmann, L., Bartenschlager, R., 1999. Replication of subgenomic hepatitis C virus RNAs in a hepatoma cell line. Science 285 (5424), 110–113.

Mercer, D.F., Schiller, D.E., Elliott, J.F., Douglas, D.N., Hao, C., Rinfret, A., Addison, W.R., Fischer, K.P., Churchill, T.A., Lakey, J.R., Tyrrell, D.L., Kneteman, N.M., 2001. Hepatitis C virus replication in mice with chimeric human livers. Nat. Med. 7 (8), 927–933.

Mita, A., Hashikura, Y., Tagawa, Y., Nakayama, J., Kawakubo, M., Miyagawa, S., 2005. Expression of Fas ligand by hepatic macrophages in patients with fulminant hepatic failure. Am. J. Gastroenterol. 100 (11), 2551–2559.

Mottola, G., Cardinali, G., Ceccacci, A., Trozzi, C., Bartholomew, L., Torrisi, M.R., Pedrazzini, E., Bonatti, S., Migliaccio, G., 2002. Hepatitis C virus nonstructural proteins are localized in a modified endoplasmic reticulum of cells expressing viral subgenomic replicons. Virology 293 (1), 31–43.

Russell, R.S., Meunier, J.C., Takikawa, S., Faulk, K., Engle, R.E., Bukh, J., Purcell, R.H., Emerson, S.U., 2008. Advantages of a single-cycle production assay to study cell culture-adaptive mutations of hepatitis C virus. Proc. Natl. Acad. Sci. U. S. A. 105 (11), 4370–4375.

Ryo, K., Kamogawa, Y., Ikeda, I., Yamauchi, K., Yonehara, S., Nagata, S., Hayashi, N., 2000. Significance of Fas antigen-mediated apoptosis in human fulminant hepatic failure. Am. J. Gastroenterol. 95 (8), 2047–2055.

Sakamoto, N., Watanabe, M., 2009. New therapeutic approaches to hepatitis C virus. J. Gastroenterol. 44 (7), 643–649.

Sakamoto, N., Yoshimura, M., Kimura, T., Toyama, K., Sekine-Osajima, Y., Watanabe, M., Muramatsu, M., 2007. Bone morphogenetic protein-7 and interferon-alpha synergistically suppress hepatitis C virus replicon. Biochem. Biophys. Res. Commun. 357 (2), 467–473.

Sekine-Osajima, Y., Sakamoto, N., Mishima, K., Nakagawa, M., Itsui, Y., Tasaka, M., Nishimura-Sakurai, Y., Chen, C.H., Kanai, T., Tsuchiya, K., Wakita, T., Enomoto, N., Watanabe, M., 2008. Development of plaque assays for hepatitis C virus-JFH1 strain and isolation of mutants with enhanced cytopathogenicity and replication capacity. Virology 371 (1), 71–85.

Shuda, M., Kondoh, N., Imazeki, N., Tanaka, K., Okada, T., Mori, K., Hada, A., Arai, M., Wakatsuki, T., Matsubara, O., Yamamoto, N., Yamamoto, M., 2003. Activation of the ATF6, XBP1 and grp78 genes in human hepatocellular carcinoma: a possible involvement of the ER stress pathway in hepatocarcinogenesis. J. Hepatol. 38 (5), 605–614.

Tanabe, Y., Sakamoto, N., Enomoto, N., Kurosaki, M., Ueda, E., Maekawa, S., Yamashiro, T., Nakagawa, M., Chen, C.H., Kanazawa, N., Watanabe, M., 2004. Synergistic inhibition of intracellular hepatitis C virus replication by combination of ribavirin and interferon-alpha. J. Infect. Dis. 189, 1129–1139.

Tasaka, M., Sakamoto, N., Itakura, Y., Nakagawa, M., Itsui, Y., Sekine-Osajima, Y., Nishimura-Sakurai, Y., Chen, C.H., Yoneyama, M., Fujita, T., Wakita, T., Maekawa, S., Enomoto, N., Watanabe, M., 2007. Hepatitis C virus non-structural proteins responsible for suppression of the RIG-I/Cardif-induced interferon response. J. Gen. Virol. 88 (Pt 12), 3323–3333.

Wakita, T., Pietschmann, T., Kato, T., Date, T., Miyamoto, M., Zhao, Z., Murthy, K., Habermann, A., Krausslich, H.G., Mizokami, M., Bartenschlager, R., Liang, T.J., 2005. Production of infectious hepatitis C virus in tissue culture from a cloned viral genome. Nat. Med. 11 (7), 791–796.

Yi, M., Bodola, F., Lemon, S.M., 2002. Subgenomic hepatitis C virus replicons inducing expression of a secreted enzymatic reporter protein. Virology 304 (2), 197–210.

Yokota, T., Sakamoto, N., Enomoto, N., Tanabe, Y., Miyagishi, M., Maekawa, S., Yi, L., Kurosaki, M., Taira, K., Watanabe, M., Mizusawa, H., 2003. Inhibition of intracellular hepatitis C virus replication by synthetic and vector-derived small interfering RNAs. EMBO Rep. 4 (6), 602–608.

Zhong, J., Gastaminza, P., Cheng, G., Kapadia, S., Kato, T., Burton, D.R., Wieland, S.F., Uprichard, S.L., Wakita, T., Chisari, F.V., 2005. Robust hepatitis C virus infection in vitro. Proc. Natl. Acad. Sci. U. S. A. 102 (26), 9294–9299.

Zhong, J., Gastaminza, P., Chung, J., Stamataki, Z., Isogawa, M., Cheng, G., McKeating, J.A., Chisari, F.V., 2006. Persistent hepatitis C virus infection in vitro: coevolution of virus and host. J. Virol. 80 (22), 11082–11093.

JOURNAL OF VIROLOGY, Sept. 2010, p. 9118–9127 Vol. 84, No. 18
0022-538X/10/$12.00 doi:10.1128/JVI.00402-10

A Disulfide-Bonded Dimer of the Core Protein of Hepatitis C Virus Is Important for Virus-Like Particle Production▽†

Yukihiro Kushima,[1,2] Takaji Wakita,[3] and Makoto Hijikata[1,2]*

Department of Viral Oncology, Institute for Virus Research, Kyoto University, Kyoto 606-8507, Japan[1]; Graduate School of Biostudies, Kyoto University, Kyoto 606-8507, Japan[2]; and Department of Virology II, National Institute of Infectious Diseases, Tokyo 162-8640, Japan[3]

Received 24 February 2010/Accepted 20 June 2010

Hepatitis C virus (HCV) core protein forms the nucleocapsid of the HCV particle. Although many functions of core protein have been reported, how the HCV particle is assembled is not well understood. Here we show that the nucleocapsid-like particle of HCV is composed of a disulfide-bonded core protein complex (dbc-complex). We also found that the disulfide-bonded dimer of the core protein (dbd-core) is formed at the endoplasmic reticulum (ER), where the core protein is initially produced and processed. Mutational analysis revealed that the cysteine residue at amino acid position 128 (Cys128) of the core protein, a highly conserved residue among almost all reported isolates, is responsible for dbd-core formation and virus-like particle production but has no effect on the replication of the HCV RNA genome or the several known functions of the core protein, including RNA binding ability and localization to the lipid droplet. The Cys128 mutant core protein showed a dominant negative effect in terms of HCV-like particle production. These results suggest that this disulfide bond is critical for the HCV virion. We also obtained the results that the dbc-complex in the nucleocapsid-like structure was sensitive to proteinase K but not trypsin digestion, suggesting that the capsid is built up of a tightly packed structure of the core protein, with its amino (N)-terminal arginine-rich region being concealed inside.

Hepatitis C virus (HCV) infection is a major cause of chronic hepatitis, liver cirrhosis, and hepatocellular carcinoma, affecting approximately 200 million people worldwide (13, 29, 44). Current treatment strategies, including interferon coupled with ribavirin, are not effective for all patients infected with HCV. An error-prone replication strategy allows HCV to undergo rapid mutational evolution in response to immune pressure and thus evade adaptive immune responses (10). New approaches to HCV therapy include the development of specifically targeted antiviral therapies for hepatitis C (STAT-Cs) which target such HCV proteins as the nonstructural 3/4A (NS3/4A), serine protease, and RNA-dependent RNA polymerase NS5B proteins (3). Despite the potent antiviral activities of some of these approaches, many resistant HCV strains have been reported after treatment with existing STAT-Cs (23, 48, 51). Therefore, identification of new targets that are common to all HCV strains and that are associated with low mutation rates is an area of active research.

HCV has a 9.6-kb, plus-strand RNA genome composed of a 5′ untranslated region (UTR), an open reading frame that encodes a single polyprotein of about 3,000 amino acids, and a 3′ UTR. The polyprotein is processed by host and viral proteases to produce three structural proteins (the core, envelope 1 [E1], and E2 proteins) and seven nonstructural proteins (the p7, NS2, NS3, NS4A, NS4B, NS5A, and NS5B proteins) (14, 16, 17, 22, 49). The HCV core protein is produced cotranslationally via carboxyl (C)-terminal cleavage to generate an immature core protein, 191 amino acids in length, on the endoplasmic reticulum (ER) (16). This protein consists of three predicted domains: the N-terminal hydrophilic domain (D1), the C-terminal hydrophobic domain (D2), and the tail domain (33), which serves as a signal peptide for the E1 protein. D1 includes a number of positively charged amino acids responsible for viral RNA binding (amino acids 1 to 75) (43) and the region involved in multimerization of the core protein via homotypic interactions (amino acids 36 to 91 and 82 to 102) (32, 40) (see Fig. S1 in the supplemental material). Hydrophobic D2 includes the region responsible for core protein association with lipid droplets (LDs; amino acids 125 to 144) (7, 18, 37), which accumulate in response to core protein production (1, 6).

Many functions of the core protein have been reported (13, 38, 50), yet because infectious HCV particles cannot be appropriately produced in currently available experimental systems, HCV particle assembly has not been elucidated to date. A cell culture system that reproduces the complete life cycle of HCV *in vitro* was developed by Wakita et al. using a cloned HCV genome (JFH1) (53). Using this system, the assembly of infectious HCV particles was found to occur near LDs and ER-derived LD-associated membranes (36, 47). Neither the structures nor the functions of the virus proteins involved in virus particle assembly are known, however. To elucidate this point, we have analyzed the biochemical characteristics of the proteins within the fraction containing the HCV particle and found a disulfide-bonded core protein complex (dbc-complex). We revealed that the disulfide-bonded dimer of core protein (dbd-core) was formed by a single cysteine residue at amino

* Corresponding author. Mailing address: Department of Viral Oncology, Institute for Virus Research, Kyoto University, 53 Kawahara-cho Shougoin, Kyoto 606-8507, Japan. Phone: 81-75-751-4046. Fax: 81-75-751-3998. E-mail: mhijikat@virus.kyoto-u.ac.jp.

† Supplemental material for this article may be found at http://jvi.asm.org/.

▽ Published ahead of print on 30 June 2010.

acid position 128 on the ER. The roles of the disulfide bond of the core protein in virus-like particle formation are discussed in this paper.

MATERIALS AND METHODS

Cell culture. Cells of the HuH-7 and HuH-7.5 human hepatoma cell lines were grown in Dulbecco's modified Eagle's medium (Nacalai Tesque, Kyoto, Japan) supplemented with 10% fetal bovine serum, 100 U/ml nonessential amino acids (Invitrogen, Carlsbad, CA), and 100 μg/ml each penicillin and streptomycin sulfate (Invitrogen).

Antibodies. The antibodies used for immunoblotting and indirect immunofluorescence analysis were specific for core protein (antibody 32-1), FLAG M2 (Sigma-Aldrich, St. Louis, MO), c-myc (Sigma-Aldrich), NS5A protein (CL1), adipocyte differentiation-related protein (ADRP; StressGen, Victoria, British, Columbia, Canada), calnexin (Calnexin-NT; StressGen), and glyceraldehyde-3-phosphate dehydrogenase (GAPDH; Chemicon, Temecula, CA). Antibodies specific for core protein (antibody 32-1) were a gift from M. Kohara (The Tokyo Metropolitan Institute of Medical Science, Tokyo, Japan). Rabbit polyclonal anti-NS5A protein CL1 antibodies have been described previously (36).

Plasmid construction. All plasmids were generated by inserting PCR-amplified fragments into expression plasmids. The plasmids, primer sequences, templates for the PCRs, and restriction enzyme sites used to construct the plasmids are listed in Table S1 in the supplemental material. Plasmids pJFH1^{E2FL} (encoding the full-length HCV genome with the FLAG epitope in the E2 hypervariable region), pJFH1^{AAA99} (encoding a NS5A mutant of JFH1^{E2FL}, resulting in noninfectious HCV particles), pJFH1$^{PP/AA}$ (encoding a core protein mutant of JFH1^{E2FL}, which allows replication in cells but prevents HCV particle production), and pcDNA3-core^{WT} (an expression plasmid encoding the full-length core protein of JFH1) have been described previously (36). Plasmid pJ6/JFH1, which contains the full-length HCV genome encoding structural proteins from the J6 strain and nonstructural proteins from the JFH1 strain, was kindly provided by Charles M. Rice (The Rockefeller University, New York, NY).

***In vitro* transcription.** RNA for transfection was synthesized as described previously (36). In brief, plasmids carrying the HCV RNA sequence were linearized with XbaI and used as templates for *in vitro* transcription with MEGAscript T7 (Ambion, Austin, TX).

Transfection. Ten micrograms of JFH1^{E2FL}, JFH1^{C128A}, JFH1^{C184A}, JFH1$^{C128/184A}$, JFH1$^{PP/AA}$, or JFH^{AAA99} and J6/JFH1 or J6/JFH1^{AAA99} RNAs were transfected into HuH-7 and HuH-7.5 cells (1.0×10^7 cells) by electroporation (260 V, 0.95 μF) using a Gene Pulser II system (Bio-Rad, Hercules, CA). Core protein expression plasmids were transfected into HuH-7 cells using Lipofectamine LTX (Invitrogen), according to the manufacturer's protocol.

HCV particle precipitation. Culture medium from HCV RNA-transfected cells were concentrated using Amicon Ultra-15 centrifugal filters with Ultracell-100 membranes (Millipore, Billerica, MA) and mixed with sucrose solution in phosphate-buffered saline (PBS) to a final sucrose concentration of 2%. This mixture was ultracentrifuged (100,000 × *g*, 4°C for 2 h), and the HCV particles were obtained as a pellet. The pellet was then suspended in culture medium for infection experiments or PBS for immunoblot analysis.

Indirect immunofluorescence analysis. Indirect immunofluorescence analyses of HCV infection and the cellular localization of the HCV proteins were performed as described previously (36).

Protease protection assay. Concentrated culture medium from JFH1^{E2FL} RNA-transfected HuH-7 cells was fractionated using 20 to 50% sucrose density gradients, and the HCV RNA titer was measured in quantitative reverse transcription-PCRs (RT-PCRs) as described below. Fractions with high HCV RNA titers were collected, and JFH1^{E2FL} particles were obtained as a pellet after ultracentrifugation (100,000 × *g*, 4°C for 2 h). The pellet was suspended in PBS and treated with 10 μg/ml trypsin or 5 μg/ml proteinase K in the presence or absence of 1% Nonidet P-40 (NP-40) at 37°C for 15 min, unless otherwise indicated. The reaction was quenched by the addition of protease inhibitor cocktail (Nacalai Tesque), followed by SDS-PAGE under nonreducing conditions and immunoblotting specific for core protein.

Immunoblot analysis. Samples were subjected to SDS-PAGE in sample buffer (62.5 mM Tris-HCl [pH 7.8], 1% SDS, 10% glycerol) with or without 5% β-mercaptoethanol (β-ME) or 50 mM dithiothreitol (DTT) for reducing and nonreducing conditions, respectively. *N*-Ethylmaleimide (NEM; Nacalai Tesque) was added to the sample buffer to a final concentration of 5 mM for the indicated samples. Proteins were transferred to a polyvinylidene difluoride membrane and blocked in blocking buffer for 1 h at room temperature with gentle agitation. After incubation with primary antibodies overnight at 4°C, the membrane was washed three times for 5 min in washing buffer at room temperature with gentle agitation. The membrane was then incubated with horseradish peroxidase (HRP)-conjugated secondary antibodies for 1 h at room temperature. After three washes in washing buffer, proteins were detected using Western Lightning reagent (PerkinElmer, Waltham, MA) or ECL Advance (GE Healthcare, Buckinghamshire, England) and Kodak MXJB Plus medical X-ray film (Kodak, Rochester, NY) or an LAS-4000 system (Fujifilm, Tokyo, Japan).

Preparation of LDs. LDs were prepared as described previously (36).

Preparation of MMFs. Microsomal membrane fractions (MMFs) were collected as described previously (15) with some modifications. In brief, cells were collected in homogenization buffer (20 mM Tris-HCl [pH 7.8], 250 mM sucrose, and 0.1% ethanol supplemented with protease inhibitor cocktail) and homogenized on ice using 40 strokes of a Dounce homogenizer. The samples were then centrifuged at 1,000 × *g* for 10 min at 4°C. The supernatant was collected in a new tube and centrifuged again at 16,000 × *g* for 20 min at 4°C. The supernatant was further centrifuged at 100,000 × *g* for 1 h at 4°C. The MMF precipitate was homogenized in lysis buffer (1% NP-40, 0.1% SDS, 20 mM Tris-HCl [pH 8.0], 150 mM NaCl, 1 mM EDTA, and 10% glycerol supplemented with protease inhibitor cocktail) using a Dounce homogenizer.

qRT-PCR analysis. Quantitative RT-PCR (qRT-PCR) analysis for determination of the HCV RNA titer was performed as described previously (36).

ELISA specific for core protein. The core protein in culture medium was quantified using an enzyme-linked immunosorbent assay (ELISA; HCV antigen ELISA; Ortho-Clinical Diagnostics, Raritan, NJ), according to the manufacturer's protocol.

RNA-protein binding precipitation assay. Core^{WT} or core^{C128A} was translated *in vitro* from pcDNA3-core^{WT} and pcDNA3-core^{C128A}, respectively, using a TNT-coupled rabbit reticulocyte lysate system (Promega, Madison, WI), according to the manufacturer's protocol. These proteins were incubated with poly(U) agarose (Sigma) in binding buffer (50 mM HEPES (pH 7.4)–100 mM NaCl–0.1% NP-40–20 U RNase inhibitor) at 4°C for 2 h with or without RNase A. After five washes, the resin-bound core proteins were immunoblotted.

RESULTS

The HCV particle contains core protein complex formed by a disulfide bond. To analyze the core protein of the HCV particle, we first subjected the concentrated culture medium of HuH-7 cells transfected with *in vitro*-transcribed JFH1^{E2FL} RNA to ultracentrifugation. After the resulting pellet was resuspended in culture medium, we confirmed the presence of infectious HCV particles on the basis of the infectivity of HuH-7.5 cells (Fig. 1a). The infectious JFH1^{E2FL} particle-containing pellet was separated by SDS-PAGE under nonreducing conditions, and immunoblot analysis showed the presence of a core antibody-reactive protein that was approximately twice the size of the core protein (38 kDa), in addition to the expected 19-kDa core protein (Fig. 1b, lane 1). Because treatment with DTT eliminated the larger core protein antibody-reactive band while the levels of the core protein monomer increased (Fig. 1b, lanes 2 to 6), the larger protein likely represented a dbc-complex. This complex was also found in J6/JFH1-derived particles (see Fig. S2 in the supplemental material), indicating that the complex was not specific for JFH1^{E2FL}.

To determine whether the dbc-complex is a component of the HCV particle, a protease protection assay was performed using RNase-resistant HCV particles fractionated on the basis of their buoyant densities. Concentrated culture medium from HuH-7 cells transfected with *in vitro*-transcribed JFH1^{E2FL} RNA was fractionated using a 20 to 50% sucrose density gradient; and JFH1^{E2FL} particles, which were presumed to contain both infectious and noninfectious particles, were collected from fractions with high HCV RNA titers using ultracentrifugation (Fig. 2a, fractions 8 to 13). The core protein from the collected fractions was analyzed by immunoblotting after SDS-

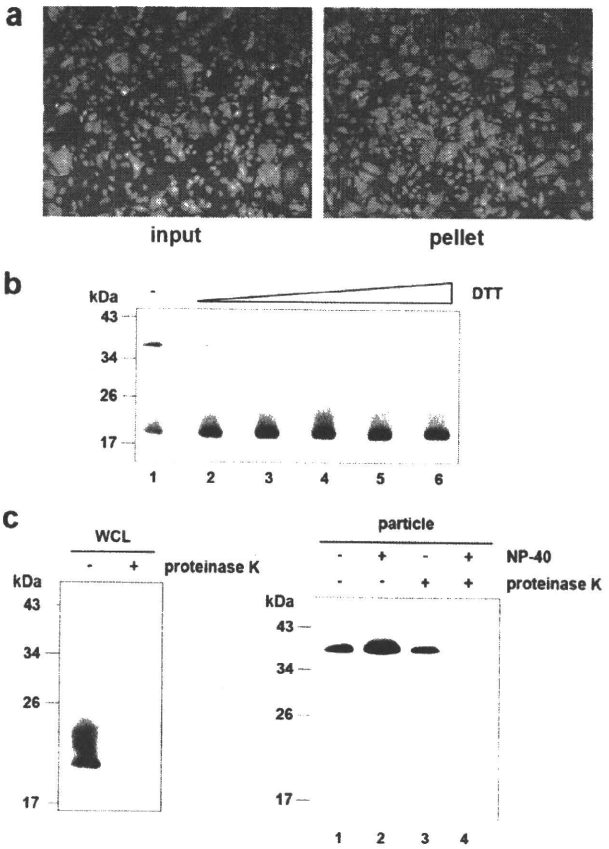

FIG. 1. The HCV-like particle consists of a core complex formed by a disulfide bond. (a) The infectivity of the pellet fraction collected from concentrated culture medium from JFH1^{E2FL} RNA-transfected HuH-7 cells was analyzed as described in Materials and Methods. Input indicates the same volume of concentrated culture medium used to pellet the virus-like particles. (b) Immunoblot analysis of the core protein in pellets containing JFH1^{E2FL} virus particles treated with various levels of DTT (lanes 1, 2, 3, 4, 5, and 6, 0, 1.56, 3.13, 6.25, 12.5, and 25 mM DTT, respectively). (c) Immunoblot analysis of the core protein in JFH1^{E2FL} particles collected from sucrose density gradient fractions with high HCV RNA titers (particle) (Fig. 2a, fractions 8 to 13) and treated with 5 μg/ml proteinase K at 37°C for 15 min in the presence or absence of 1% NP-40 (right panel). As a positive control, WCL prepared from JFH1^{E2FL} RNA-transfected HuH-7 cells in lysis buffer was treated with 5 μg/ml proteinase K at 37°C for 15 min (left panel). Data are representative of three independent experiments.

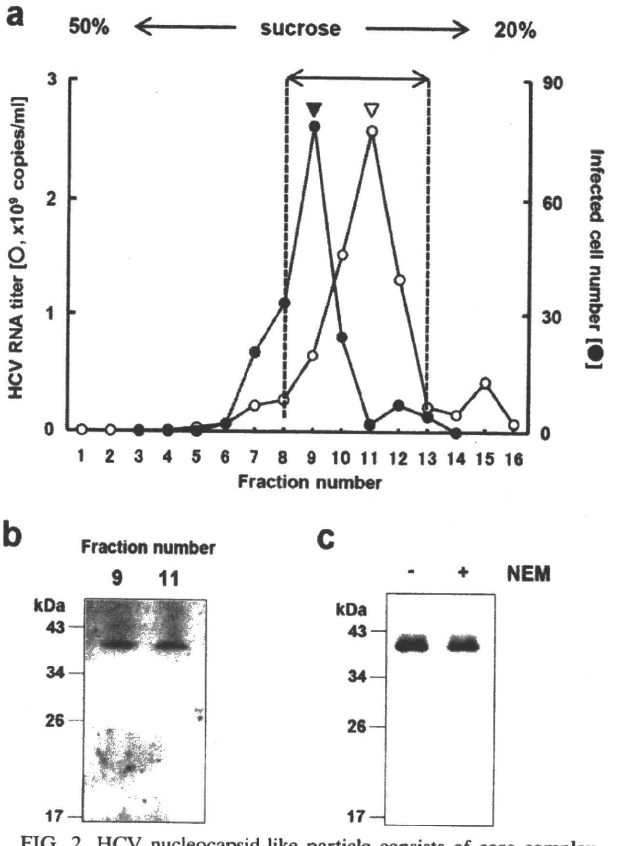

FIG. 2. HCV nucleocapsid-like particle consists of core complex. (a) HCV RNA titer in culture medium separated on a 20 to 50% sucrose density gradient. Concentrated culture medium from JFH1^{E2FL} RNA-transfected HuH-7 cells were treated with RNase and separated on a 20 to 50% sucrose density gradient. Fractions 1 to 16 were obtained from the bottom to the top of the tube, respectively. The HCV RNA titer and infectivity of each fraction were analyzed by real-time qRT-PCR (for fractions 1 to 16) and counting the number of cells infected with HCV-like particle detected by immunofluorescence (for fractions 3 to 14), respectively, as described in Materials and Methods. In brief, each fraction was diluted with 1× PBS and HCV-like particles were collected by ultracentrifugation, and then the pellets were suspended in culture medium and used for infection. (b) HCV-like particle collected from the infectious HCV peak (from panel a, filled arrowhead) and the HCV RNA peak (from panel a, open arrowhead) were collected by ultracentrifugation, subjected to nonreducing SDS-PAGE, and detected by immunoblotting against the core protein. (c) HCV-like particles collected from fractions 8 to 13 (a) were subjected to nonreducing SDS-PAGE in the presence (lane +) or absence (lane −) of 5 mM NEM and analyzed by immunoblotting against the core protein. Data are representative of two (a, infectivity of fractions) or three independent experiments.

PAGE under nonreducing conditions and showed only the dbc-complex (Fig. 1c, right panel).

To examine whether the complex contributes to the infectivity of the particles, we analyzed the dbc-complex in the fractions containing infectious and noninfectious HCV particles (fractions 9 and 11 of Fig. 2a, filled and open arrowheads, respectively). Both the infectious and noninfectious HCV particle-containing fractions contained the dbc-complex (Fig. 2b). To confirm this further, a pellet containing particles of mutant JFH1$^{\Delta\Delta\Delta 99}$—a mutant of JFH1^{E2FL} that primarily produces noninfectious particles (36)—was analyzed in a similar manner. These dbc-complexes were found in pelleted particles of both JFH1$^{\Delta\Delta\Delta 99}$ and J6/JFH1$^{\Delta\Delta\Delta 99}$, which was a mutant J6/JFH1 with a similar substitution to JFH1$^{\Delta\Delta\Delta 99}$ (see Fig. S2 in the supplemental material). These results indicated that the dbc-complex was present in both the infectious and noninfectious HCV-like particles.

The core protein monomer observed in the pellet samples (Fig. 1b) may be from the secreted core protein or the debris of apoptotic cells, because the core protein is known to be secreted from cells expressing this protein under particular conditions (42) and strain JFH1 is known to cause apoptosis (45). The dbc-complex-specific signals in the HCV particles seem to be increased in the NP-40-treated samples for some

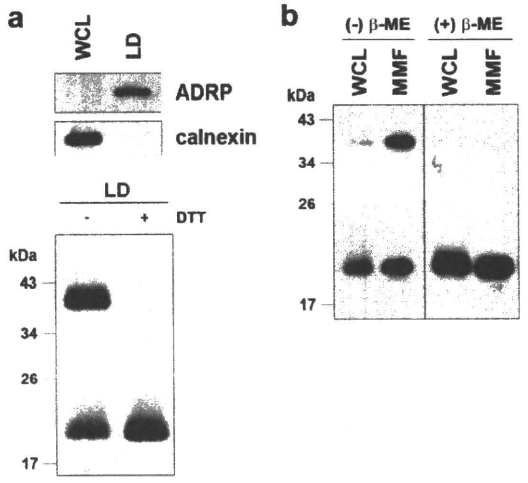

FIG. 3. The core complex is formed at the LD and ER. (a) The LD fraction and WCL were collected from JFH1^{E2FL} RNA-transfected HuH-7 cells on day 5 posttransfection. (upper panel) Immunoblot analysis of the LD marker ADRP and the ER marker calnexin in the LD fraction; (lower panel) immunoblot analysis of the core protein in the LD fraction treated or not treated with 50 mM DTT. (b) Immunoblot analysis of the core protein in the MMF and WCL collected from JFH1^{E2FL}-producing HuH-7 cells on day 5 posttransfection in the presence or absence of 5% β-ME. Data are representative of those from three independent experiments.

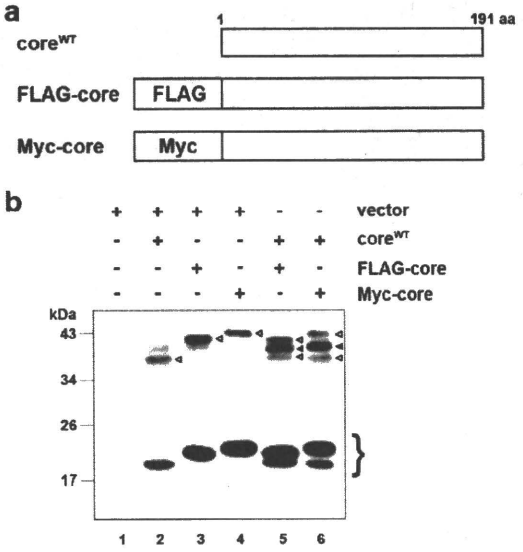

FIG. 4. The core complex consists of a core dimer. (a) Schematic of wild-type, FLAG-tagged (FLAG-core), and Myc-tagged (Myc-core) core proteins. (b) Immunoblot analysis of the core protein in the MMF collected from HuH-7 cells transfected with combinations of pcDNA3 (vector) and/or core expression plasmids (e.g., encoding core^{WT}, FLAG-core, and Myc-core), as indicated. The experiment was performed under nonreducing conditions. The lower bands represent core monomer (marked on the right with a brace). White arrowheads, bands corresponding to dbd-core; black arrowheads, positions of the intermediately sized core complex formed by core^{WT} and the tagged core. Data are representative of those from three independent experiments.

unknown reason (Fig. 1c, lanes 1 and 2). Although the intermolecular disulfide bond is known to be artificially formed in denaturing SDS-PAGE in the absence of reducing agents, the dbc-complex was still observed even in the presence of NEM, which is the alkylating agent for free sulfhydryls, during sample preparation (Fig. 2c), indicating that the dbc-complex was naturally present in the virus-like particles.

The HCV nucleocapsid is covered with lipid membranes and E1 and E2 proteins, making it resistant to proteases. As expected, in the absence of NP-40, the dbc-complex was resistant to proteinase K (Fig. 1c, lane 3), whereas proteinase K was able to digest core protein in whole-cell lysates (WCLs) collected from JFH1^{E2FL}-transfected HuH-7 cells (Fig. 1c, left panel). Disrupting the envelope structure with NP-40 made the dbc-complex susceptible to proteinase K treatment (Fig. 1c, lane 4), indicating that the dbc-complex was indeed a component of the HCV particle.

The dbc-complex forms on the ER. To investigate the subcellular site at which the dbc-complex forms, LDs and MMFs from JFH1^{E2FL} replicating HuH-7 cells were analyzed by immunoblotting. We first analyzed the dbc-complex in LDs, because LDs are involved in infectious HCV particle formation (36, 47). The purity of the LD fraction was determined using immunoblot analysis of calnexin and ADRP, ER and LD marker proteins, respectively (Fig. 3a, upper panel). The core protein was then analyzed in the LD fraction. As shown in Fig. 3a (lower panel), the dbc-complex was observed in the LD fraction from JFH1^{E2FL} RNA-transfected HuH-7 cells. We next analyzed the core protein in the ER-containing MMF, because the core protein is first translated and processed on the ER (16). As shown in Fig. 3b, the dbc-complex was observed in the MMF from JFH1^{E2FL} RNA-transfected HuH-7 cells. These results suggest that the dbc-complex is first formed at the ER. To assess the possibility that dbc-complex-containing HCV particles were also assembled on the ER, the sensitivity of the dbc-complex to protease treatment was analyzed. The dbc-complex in the MMF was susceptible to protease treatment in the absence of NP-40, indicating that the dbc-complex on the ER was not yet part of a HCV particle (data not shown).

dbc-complex is most likely a disulfide-bonded dimer form of the core. In order to examine whether the core protein itself has the potential to form a dbc-complex, we analyzed the dbc-complex formation of the full-length wild-type core protein (core^{WT}) expressed from pcDNA3-core^{WT} (36), the expression plasmid encoding the 191-amino-acid full-length core protein of JFH1 strain. We used this expression plasmid because the core protein from this plasmid was likely to be processed correctly enough to produce infectious HCV particles when it was cotransfected with the RNA of JFH1^{dc3}, which is a core protein deletion mutant of JFH1 (36). As a result, the dbc-complex formation was observed from the MMF of core^{WT}-expressing cells both in the absence and in the presence of NEM (Fig. 4b; lane 2 and data not shown, respectively). We next investigated the effect of the amino acid region of E1 on the production of the dbc-complex, because it has been reported that the efficient processing of core protein is dependent on the presence of some E1 sequence to ensure the insertion of the signal sequence for E1 in the translocon/membrane machinery (34). The dbc-complex was also observed

when the core protein was expressed from pcDNA3-C-E1/25, which encodes the full-length core protein followed by the N-terminal 25-amino-acid sequence of E1 to ensure that the core protein is processed properly (see Fig. S3a in the supplemental material). These data showed that the dbc-complex was formed by expression of the core protein only in the cells.

Next, we examined the structural components of the dbc-complex. Because the dbc-complex was twice the size of the core protein monomer, it was likely dbd-core. So, we investigated whether the core protein molecules with different tags were able to form the dbd-core. We first generated expression plasmids encoding core protein with the N-terminal FLAG and Myc tags (pcDNA3-FLAG-core and pcDNA3-Myc-core, respectively; Fig. 4a). The tagged core proteins were expressed or coexpressed with $core^{WT}$ in HuH-7 cells, and the MMF was analyzed by immunoblotting. The FLAG or Myc tag shifted the positions of the monomer and the complex bands (Fig. 4b, lanes 3 and 4) compared with the position of $core^{WT}$ (Fig. 4b, lane 2). When $core^{WT}$ was coexpressed with FLAG-core or Myc-core, the core protein complex of an intermediate size was observed, in addition to the bands obtained when the constructs were independently expressed (Fig. 4b, lanes 5 and 6, filled arrowheads); the intermediate-sized band disappeared after treatment with β-ME (see Fig. S3b, lanes 11 and 12, filled arrows, in the supplemental material), indicating that $core^{WT}$ and tagged core protein formed a heteromeric disulfide-bonded dimer. These results demonstrated that the dbc-complex on the ER is a dbd-core. Although we tried to detect the hetero- or homodimer consisting of the tagged core protein by using anti-FLAG or anti-Myc antibodies, these dimers were not detected, possibly because of the lower levels of sensitivity and specificity of the antibodies compared to those of the anti-core protein antibody that we used, especially against epitopes in the dbd-core. The results presented above, coupled with the similarities of the molecular sizes and sensitivities to β-ME and DTT, suggested that the dbc-complex in the HCV particle is most likely a dbd-core.

Core protein Cys128 mediates dbd-core formation. Our results showed that core protein from $JFH1^{E2FL}$ forms a disulfide-bonded dimer on the ER. A search for cysteine residues in the $JFH1^{E2FL}$ core protein identified amino acid positions 128 (Cys128) and 184 (Cys184) (see Fig. S1 in the supplemental material). These residues are highly conserved in core proteins from the approximately 2,000 reported HCV strains (HCVdb, http://www.hcvdb.org/, Hepatitis C Virus Database; http://s2as02.genes.nig.ac.jp/). To determine which cysteine residue mediated disulfide bond formation, we generated point mutations in $JFH1^{E2FL}$ that replaced Cys128 and/or Cys184 with alanine (Ala) (C128A, C184A, and C128/184A in $JFH1^{C128A}$, $JFH1^{C184A}$, and $JFH1^{C128/184A}$, respectively; Fig. 5a). As shown in Fig. 5b, the core proteins from $JFH1^{C128A}$ and $JFH1^{C128/184A}$ failed to form a dbd-core under nonreducing condition, whereas the core protein from $JFH1^{C184A}$ formed the dimer, indicating that Cys128 was the residue responsible. Similar results were observed when Cys was replaced by serine (Ser) instead of Ala (see Fig. S5c in the supplemental material). Recently, Majeau et al. reported that the core protein of the J6/JFH1 strain with Cys128 replacements by Ala or Ser were unstable in both *Pichia pastoris* and human hepatoma cell line HuH-7.5 (31), although we did not detect any noticeable degradation of the mutant core proteins of strain JFH1 (Fig. 5b; see also Fig. S5c in the supplemental material). This difference may have resulted from the difference in sample preparation methods, as we used the full-length genome of $JFH1^{E2FL}$ strain bearing the strain JFH1 core protein and HuH-7 cells instead of a core protein-expressing plasmid for the J6 strain and HuH-7.5 cells.

To exclude the possibility that mutation of Cys128 inhibited dbd-core formation by creating a conformational change, T127A and G129A core protein mutants ($JFH1^{T127A}$ and $JHF1^{G129A}$, respectively) were created and examined for their effects on dbd-core formation and infectious virus particle production. These mutants formed dbd-core, and infectious HCV particles were detected in the culture medium (see Fig. S4a to c in the supplemental material), supporting an essential role for Cys128 in dbd-core and particle formation.

dbd-core contributes to HCV particle production. To examine the functional roles of dbd-core, infectious HCV particle production, HCV replication efficiency, colocalization of the core protein and LDs, and RNA binding of mutant and wild-type ($JFH1^{E2FL}$) core protein were evaluated. Culture medium from HuH-7 cells transfected with $JFH1^{C128A}$ or $JFH1^{C128/184A}$ RNA contained significantly fewer infectious HCV particles compared with the numbers obtained with $JFH1^{E2FL}$ or $JFH1^{C184A}$ RNA (Fig. 5c). We also found significant decreases in the levels of HCV RNA and core protein in the culture medium of HuH-7 cells transfected with $JFH1^{C128A}$ or $JFH1^{C128/184A}$ RNA (Fig. 5d and e). Similar results were observed with J6/JFH1 C128A or the C128/184A mutant strain (data not shown). To investigate whether these results were due to suppressed HCV replication, the HCV RNA and protein levels in cells transfected with mutant RNA were analyzed using qRT-PCR and immunoblot analyses, respectively. Compared with the results obtained with $JFH1^{E2FL}$, no significant changes in the cellular HCV RNA titer at days 1, 3, and 5 posttransfection or in the expression of HCV nonstructural protein NS5A were observed (Fig. 6a and b). This indicated that substitution of Cys128 did not significantly affect HCV RNA genome replication or viral protein production, demonstrating that the dbd-core functions during HCV particle production rather than HCV genome replication. Similar results were observed using RNA of JFH1 mutant strain $JFH1^{C128S}$, in which the cysteine at position 128 was replaced by Ser instead of Ala (see Fig. S5a, b, and d in the supplemental material).

The subcellular localizations of the core protein and NS5A protein in HuH-7 cells transfected with HCV RNA were investigated using indirect immunofluorescence and confocal microscopy, because recruiting HCV proteins to LDs is an important step in infectious HCV particle production (36, 47) and core trafficking to LDs is dependent on signal peptide peptidase (SPP)-mediated cleavage of the tail region (34, 41). $JFH1^{C128A}$ mutant core protein and NS5A protein were efficiently trafficked to LDs, as was observed with wild-type $JHF1^{E2FL}$ (Fig. 6c), suggesting that SPP cleavage and core protein maturation were not affected by the C128A mutation. Similar results were obtained with the core proteins derived from $JFH1^{C184A}$ and $JFH1^{C128/184A}$ (see Fig. S6 in the supplemental material) and also Ser mutant $JFH1^{C128S}$ (see Fig. 5e in the supplemental material).

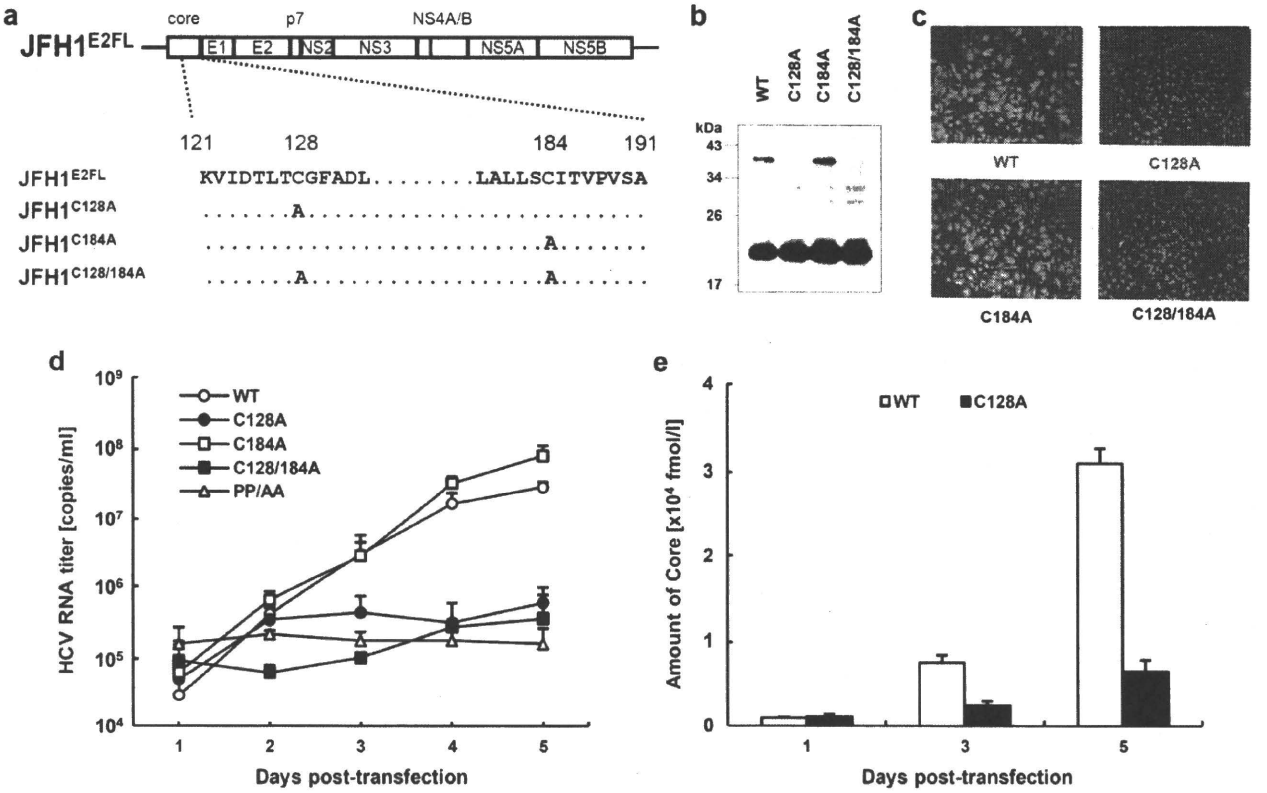

FIG. 5. The core dimer is formed via a bond between cysteine residues at amino acid position 128. (a) Site-directed mutagenesis of JFH1^{E2FL}. (b) Immunoblot analysis of the core protein in MMFs collected from HuH-7 cells under nonreducing conditions 3 days post-transfection with JFH1^{E2FL} (WT), JFH1^{C128A} (C128A), JFH1^{C184A} (C184A), or JFH1$^{C128/184A}$ (C128/184A) RNA. (c) Infectivity of culture medium collected and concentrated on day 5 posttransfection from HuH-7 cells transfected with WT, C128A, C184A, or C128/184A RNA. (d) Real-time qRT-PCR analysis of HCV RNA titers in culture medium collected at the indicated time points from HuH-7 cells transfected with WT, C128A, C184A, C128/184A, or PP/AA (JFH1$^{PP/AA}$) RNA. (e) ELISAs of core protein levels in culture medium collected at the indicated time points from HuH-7 cells transfected with WT or C128A RNA. Data are representative of those from three independent experiments (b and c) or are the means ± standard deviations from three independent experiments (d and e).

Because HCV core protein can bind to RNA, including the HCV genome, during viral particle assembly (43), we analyzed RNA binding by the core protein using *in vitro*-translated core^{C128A}, core^{WT}, and poly(U) agarose resin. Core^{C128A} and core^{WT} bound similarly to the poly(U) resin (Fig. 6d).

dbd-core is important for HCV particle assembly. The mutational analysis of the core protein indicated that core^{C128A} and core^{WT} similarly localize to LDs, recruit NS proteins to the LD, and bind to RNA. Moreover, this mutation did not markedly affect HCV genome replication. How does core^{C128A} affect the production of HCV particles? An important function of the core protein is multimerization, which is followed by capsid construction and packaging of the RNA genome in the viral particles. We therefore determined whether core^{C128A} had a dominant negative effect on virus-like particle production. Wild-type JFH1^{E2FL} RNA and different amounts of JFH1^{C128A} RNA were cotransfected into HuH-7 cells, and the HCV RNA titer and infectivity of the virus-like particles in the culture medium were analyzed. As expected, the HCV RNA titer in the cells increased with higher levels of transfected RNA (see Fig. S7a in the supplemental material). In contrast, the HCV RNA titer and infectivity in the culture medium decreased in a JFH1^{C128A} RNA dose-dependent manner when this mutant RNA was cotransfected with wild-type RNA (Fig. 7a, b). This suppressive effect was not observed when either wild-type RNA or core deletion mutant JFH1^{dc3} RNA was used instead of mutant RNA in a similar experiment (see Fig. S7b to e in the supplemental material), indicating that higher levels of HCV RNA alone did not inhibit HCV particle production. Thus, core^{C128A} had a dominant negative effect on HCV particle production. Together, these results suggest that dbd-core is involved in the assembly of HCV particles.

The nucleocapsid-like particle of HCV was resistant to trypsin treatment. To further investigate the structure of the HCV nucleocapsid-like particle most likely formed by dbd-core, we examined the sensitivity of the particle to trypsin, which cleaves polypeptides at the C-terminal end of basic residues. Whereas trypsin digested the core protein in the whole-cell lysates (Fig. 8a, left panel), dbd-core from buoyant density-fractionated JFH1^{E2FL} particles was resistant to digestion, despite NP-40 treatment (Fig. 8a, right panel), although it was sensitive to proteinase K, which has a broad specificity (Fig. 1c). The N-terminal hydrophilic domain of the core protein (from residues 6 to 121) contains a number of trypsin cleavage sites (25 sites

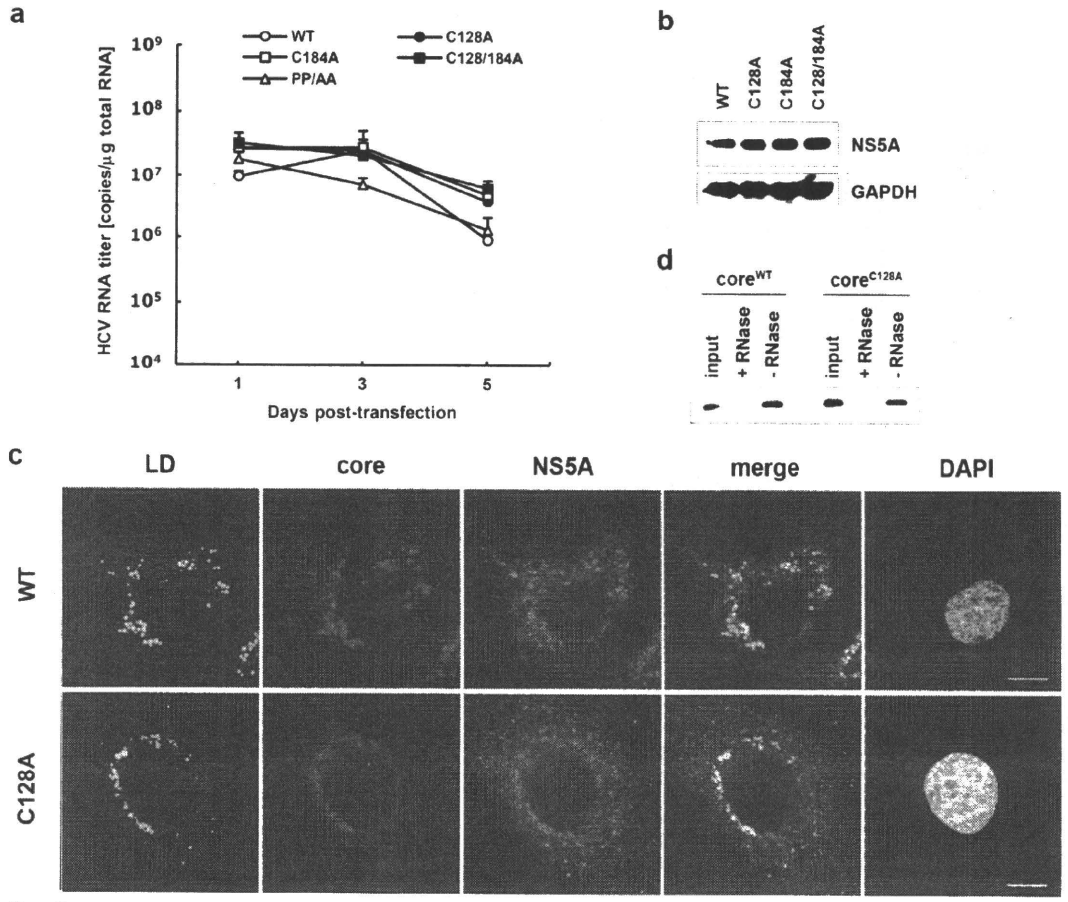

FIG. 6. Site-directed mutagenesis has no effect on HCV replication. (a) Real-time qRT-PCR analysis of the HCV RNA titer using total cellular RNA collected at the indicated time points from cells transfected with $JFH1^{J/2FL}$ (WT), $JFH1^{C128A}$ (C128A), $JFH1^{C184A}$ (C184A), $JFH1^{C128/184A}$ (C128/184A), or $JFH1^{PP/AA}$ (PP/AA) RNA. (b) Immunoblot analysis of NS5A protein and GAPDH in whole-cell lysate collected from cells transfected with WT, C128A, C184A, or C128/184A RNA at day 3 posttransfection. (c) Confocal microscopy of the subcellular localization of the LD (green), core (blue), NS5A protein (red), and nucleus (4′,6-diamidino-2-phenylindole [DAPI]) (gray) in WT and C128A replicating cells on day 3 posttransfection. Bars, 10 μm. (d) An RNA-protein binding precipitation assay was performed with *in vitro*-translated $core^{WT}$ and $core^{C128A}$ using poly(U) agarose as the resin. +RNase and −RNase, samples with and without RNase treatment, respectively, as described in Materials and Methods. Input indicates that 1/40 of the amount of translated product was used in this assay. Data represent the means ± standard deviations from three independent experiments (a) or are representative of those from three independent experiments (b to d).

in strain JHF1) (see Fig. S1 in the supplemental material), suggesting that the N-terminal domain faces inward and/or that the conformation prevents protease access. To address this idea, buoyant density-fractionated $JFH1^{J/2FL}$ particles were treated with trypsin under stricter conditions in the presence of NP-40. Cleavage of dbd-core by various levels of trypsin correlated with the appearance of a shorter molecule (Fig. 8b, white arrowhead). The shorter molecule was presumed to be partially digested dbd-core with an intact N-terminal region because it was recognized by anti-core protein antibodies, which bind to an epitope located from amino acids 20 to 40 of the core protein (M. Kohara, The Tokyo Metropolitan Institute of Medical Science, personal communication). These results suggest that dbd-core is assembled into the nucleocapsid-like particle such that most of the N-terminal domain is inside.

DISCUSSION

In the present study, we have shown that the nucleocapsid-like particle of HCV most likely contains a dimer of core protein that is stabilized by a disulfide bond. Mutational analysis revealed that Cys128 forms a disulfide bond between core monomers. Several reports have shown that disulfide bonds in the capsid proteins of some viruses are involved in virus particle assembly and stabilization of the viral capsid structure (4, 21, 27, 28, 57); these viruses are characterized by icosahedral nucleocapsids. Because, like these viruses, the HCV virion is spherical (2, 20), it has been suggested that HCV may contain a nucleocapsid with a similar structure (20). We found the dbc-complex, which is most likely to be the dbd-core in $JFH1^{J/2FL}$ virus-like particles (Fig. 1c and 8a). The dbd-core in the capsid structure was digested by proteinase K but not

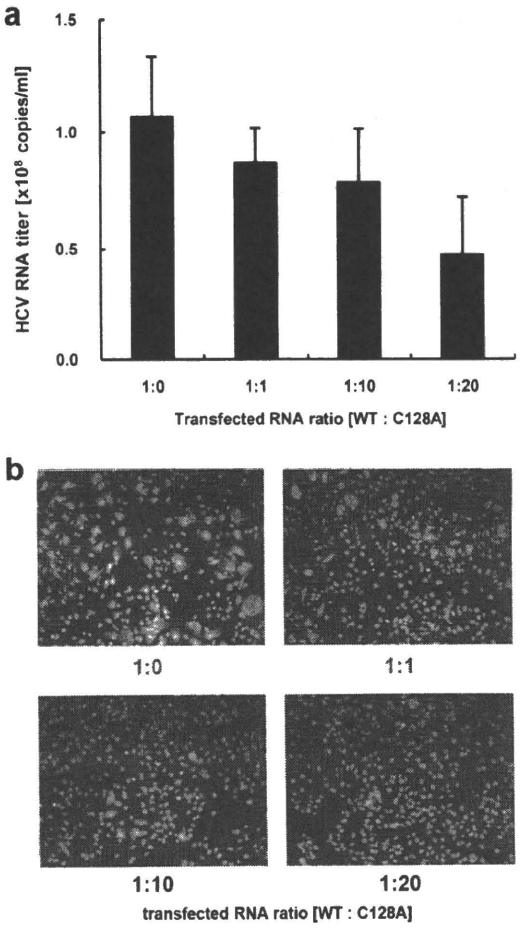

FIG. 7. JFH1^{C128A} core inhibits JFH1^{E2FL} particle assembly. A competitive inhibitory assay was performed with JFH1^{E2FL} (WT) and JFH1^{C128A} (C128A). (a) Real-time qRT-PCR analysis of the HCV RNA titer in HuH-7 cell culture medium 3 days after the cells were transfected with the indicated ratio of WT and C128A RNA. (b) The infectivity of culture medium collected from HuH-7 cells that had been transfected with the indicated ratio of WT and C128A RNA was analyzed as described in Materials and Methods. Data represent the means ± standard deviations from three independent experiments (a) or are representative of those from three independent experiments (b).

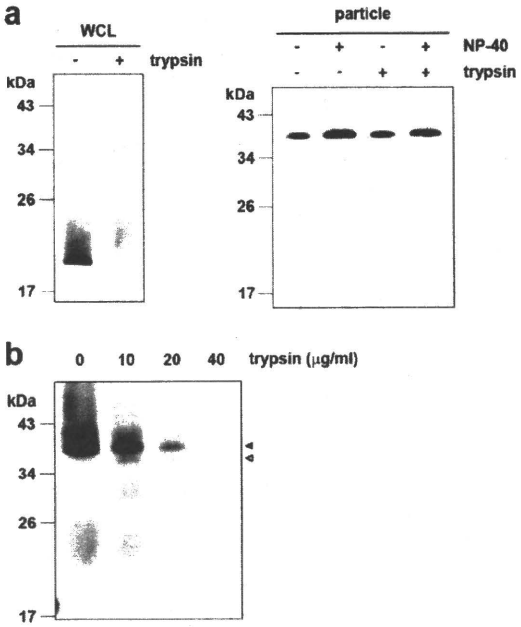

FIG. 8. The nucleocapsid-like particle of JFH1^{E2FL} is assembled with the C-terminal region of the core protein on the outer surface. (a) Immunoblot analysis of the core protein in JFH1^{E2FL} particles collected from sucrose density gradient fractions with high HCV RNA titers (particle) (Fig. 2a, fractions 8 to 13). The fractions were treated with 10 μg/ml trypsin at 37°C for 15 min in the presence or absence of 1% NP-40 (right panel). As a positive control, WCL prepared from JFH1^{E2FL} RNA-transfected HuH-7 cells in lysis buffer was treated with 10 μg/ml trypsin at 37°C for 15 min (left panel). (b) Immunoblot analysis of the core protein in JFH1^{E2FL} particles collected from sucrose density gradient fractions with high HCV RNA titers (Fig. 2a, fractions 8 to 13). The fractions were treated with the indicated concentrations of trypsin at 37°C for 10 min in the presence of 1% NP-40. Open and filled arrows indicate the positions of dbd-core and the trypsin-digested fragment, respectively. Data are representative of those from three independent experiments.

trypsin in the presence of NP-40 (Fig. 1c and 8a, lane 4). The resistance to trypsin suggested a tight conformation for dbd-core in the capsid and no exposed trypsin cleavage sites. The truncated form of dbd-core that was observed under certain trypsin treatment conditions likely resulted from cleavage in the C-terminal portion of the protein (e.g., arginine residues at positions 149 and 156) (see Fig. S1 in the supplemental material), although it is possible that the truncation of dbd-core was due to nonspecific cleavage by trypsin. These results imply that dbd-core is configured such that the N- and C-terminal ends are located at the inner and outer surfaces of the capsid, respectively. Because the N-terminal region of the core protein includes the RNA binding domain (43), the HCV RNA genome likely interacts with the core protein as it is packed in the nucleocapsid. On the other hand, the C-terminal hydrophobic domain probably faces the lipid membranes to form the envelope structure. Only part of the N-terminal hydrophilic region of the core protein has been structurally examined using X-ray crystal structural analysis (35) and structural bioinformatics and nuclear magnetic resonance analysis (11). Although the C-terminal half of the core protein has been structurally investigated by the use of bioinformatics (8), the three-dimensional structure containing the Cys128 residue is unknown. Thus, determination of the structure of the core protein in the nucleocapsid containing the Cys128 residue should be required for understanding the whole structure of this protein in the virus particles.

Because cotransfection of JFH1^{C128A} RNA with wild-type JFH1^{E2FL} RNA inhibited particle production in a mutant RNA dose-dependent manner (Fig. 7a and b), the C128A core variant clearly inhibited HCV particle formation by wild-type core protein. Cys128 was also previously reported to be a residue included in the region important for the production of infectious HCV (39). This residue is located near the N-terminal end of the hydrophobic region of the core (amino acids 122 to 177) and belongs to the hydrophilic side of an amphipathic helix expected to interact in the plane of the membrane interface (7). Therefore, it is possible to think that dbd-core

formation via Cys128 can stabilize the interaction between the core protein and the membranes. The N-terminal half of the core protein (amino acids 1 to 124) reportedly assembles into nucleocapsid-like particles in the presence of the 5′ UTR from HCV RNA (24), suggesting that some nucleocapsid-like particles may assemble via only homotypic interactions from the core protein. In addition to weak homotypic interactions, the HCV core protein forms a disulfide bond to stabilize the capsid structure, thus making dbd-core indispensable in the stable virus-like particle. We observed that culture medium from JFH1^{C128A}- or JFH1^{C128S}-transfected cells included slight infectivity (Fig. 5c; see also Fig. S5d in the supplemental material). This made us speculate that this mutant may produce some infective particle-like structure formed by a homotypic interaction of the core. Such a slight infectivity may have reflected the optimized *in vitro* culture conditions compared with the *in vivo* conditions, allowing relatively unstable virus particles to survive.

A nucleocapsid must be resistant to environmental degradation yet still be able to disassemble after infection. Disulfide bonds could help with this process by switching between a stable and unstable virus capsid on the basis of different intracellular and extracellular oxidation conditions (12, 30). During the virus life cycle, the disulfide bond strengthens the viral capsid structure and protects the viral genome from oxidative conditions and cellular nucleases when virus particles are formed. Upon infection, the disulfide bond may be cleaved under cytoplasmic reducing conditions, thereby releasing the viral genome into the cell for replication. HCV may utilize the core protein disulfide bond in this way as HCV enters the host cell via clathrin-mediated endocytosis (5) into a low-pH, endosomal compartment (25, 52); this is presumably followed by endosomal membrane fusion and release of the viral capsid into the cytoplasm (38).

Treatment of HCV infection with pegylated interferon in combination with ribavirin is not effective for all patients. Recently, drugs targeting viral proteins NS3/4A and NS5B have been examined in clinical trials. Although these drugs are relatively specific, resulting in fewer side effects and potent antiviral activity, monotherapy can be complicated by rapidly emerging resistant variants carrying mutations that reduce drug efficacy, perhaps due to conformational changes in the target (23, 48, 51). Therefore, viral proteins that are highly conserved among strains and those characterized by low mutation rates may be better targets for drug development. Because the core protein is the most conserved HCV protein and Cys128 is conserved among almost all HCV strains examined, drugs that interact with Cys128 and/or the region around or near this residue will likely show broad-spectrum efficacy to block stable infectious particle formation. Structural analysis of dbd-core should aid with the development of new STAT-Cs that target Cys128 by direct interaction with the sulfide group and/or region around this residue. Until now and still, the mechanism of disulfide bond formation of the core protein on the ER is unknown. Dimerization of the capsid protein by disulfide bond has been reported in some enveloped viruses (9, 19, 54, 56), although some were shown not to be important for virus particle formation (26, 55). Unlike vaccinia virus (46), no redox system of its own has been reported for these viruses. Therefore, further investigations addressing the mechanisms underlying dbd-core formation on the ER may reveal a new mechanism for disulfide bond formation of viral proteins in infected cells.

ACKNOWLEDGMENTS

This work was supported by grants-in-aid from the Ministry of Health, Labor, and Welfare of Japan and by grants-in-aid from the Japan Health Sciences Foundation.

REFERENCES

1. **Abid, K., V. Pazienza, A. de Gottardi, L. Rubbia-Brandt, B. Conne, P. Pugnale, C. Rossi, A. Mangia, and F. Negro.** 2005. An in vitro model of hepatitis C virus genotype 3a-associated triglycerides accumulation. J. Hepatol. **42**:744–751.
2. **Aly, H. H., Y. Qi, K. Atsuzawa, N. Usuda, Y. Takada, M. Mizokami, K. Shimotohno, and M. Hijikata.** 2009. Strain-dependent viral dynamics and virus-cell interactions in a novel in vitro system supporting the life cycle of blood-borne hepatitis C virus. Hepatology **50**:689–696.
3. **Asselah, T., Y. Benhamou, and P. Marcellin.** 2009. Protease and polymerase inhibitors for the treatment of hepatitis C. Liver Int. **29**(Suppl. 1):57–67.
4. **Baron, M. D., and K. Forsell.** 1991. Oligomerization of the structural proteins of rubella virus. Virology **185**:811–819.
5. **Blanchard, E., S. Belouzard, L. Goueslain, T. Wakita, J. Dubuisson, C. Wychowski, and Y. Rouille.** 2006. Hepatitis C virus entry depends on clathrin-mediated endocytosis. J. Virol. **80**:6964–6972.
6. **Boulant, S., M. W. Douglas, L. Moody, A. Budkowska, P. Targett-Adams, and J. McLauchlan.** 2008. Hepatitis C virus core protein induces lipid droplet redistribution in a microtubule- and dynein-dependent manner. Traffic **9**:1268–1282.
7. **Boulant, S., R. Montserret, R. G. Hope, M. Ratinier, P. Targett-Adams, J. P. Lavergne, F. Penin, and J. McLauchlan.** 2006. Structural determinants that target the hepatitis C virus core protein to lipid droplets. J. Biol. Chem. **281**:22236–22247.
8. **Boulant, S., C. Vanbelle, C. Ebel, F. Penin, and J. P. Lavergne.** 2005. Hepatitis C virus core protein is a dimeric alpha-helical protein exhibiting membrane protein features. J. Virol. **79**:11353–11365.
9. **Cornillez-Ty, C. T., and D. W. Lazinski.** 2003. Determination of the multimerization state of the hepatitis delta virus antigens in vivo. J. Virol. **77**:10314–10326.
10. **Dustin, L. B., and C. M. Rice.** 2007. Flying under the radar: the immunobiology of hepatitis C. Annu. Rev. Immunol. **25**:71–99.
11. **Duvignaud, J. B., C. Savard, R. Fromentin, N. Majeau, D. Leclerc, and S. M. Gagne.** 2009. Structure and dynamics of the N-terminal half of hepatitis C virus core protein: an intrinsically unstructured protein. Biochem. Biophys. Res. Commun. **378**:27–31.
12. **Freedman, R. B., B. E. Brockway, and N. Lambert.** 1984. Protein disulphide-isomerase and the formation of native disulphide bonds. Biochem. Soc. Trans. **12**:929–932.
13. **Giannini, C., and C. Brechot.** 2003. Hepatitis C virus biology. Cell Death Differ. **10**(Suppl. 1):S27–S38.
14. **Grakoui, A., C. Wychowski, C. Lin, S. M. Feinstone, and C. M. Rice.** 1993. Expression and identification of hepatitis C virus polyprotein cleavage products. J. Virol. **67**:1385–1395.
15. **Higashi, Y., H. Itabe, H. Fukase, M. Mori, Y. Fujimoto, R. Sato, T. Imanaka, and T. Takano.** 2002. Distribution of microsomal triglyceride transfer protein within sub-endoplasmic reticulum regions in human hepatoma cells. Biochim. Biophys. Acta **1581**:127–136.
16. **Hijikata, M., N. Kato, Y. Ootsuyama, M. Nakagawa, and K. Shimotohno.** 1991. Gene mapping of the putative structural region of the hepatitis C virus genome by in vitro processing analysis. Proc. Natl. Acad. Sci. U. S. A. **88**:5547–5551.
17. **Hijikata, M., H. Mizushima, Y. Tanji, Y. Komoda, Y. Hirowatari, T. Akagi, N. Kato, K. Kimura, and K. Shimotohno.** 1993. Proteolytic processing and membrane association of putative nonstructural proteins of hepatitis C virus. Proc. Natl. Acad. Sci. U. S. A. **90**:10773–10777.
18. **Hope, R. G., and J. McLauchlan.** 2000. Sequence motifs required for lipid droplet association and protein stability are unique to the hepatitis C virus core protein. J. Gen. Virol. **81**:1913–1925.
19. **Hu, H. M., K. N. Shih, and S. J. Lo.** 1996. Disulfide bond formation of the in vitro-translated large antigen of hepatitis D virus. J. Virol. Methods **60**:39–46.
20. **Ishida, S., M. Kaito, M. Kohara, K. Tsukiyama-Kohora, N. Fujita, J. Ikoma, Y. Adachi, and S. Watanabe.** 2001. Hepatitis C virus core particle detected by immunoelectron microscopy and optical rotation technique. Hepatol. Res. **20**:335–347.
21. **Jeng, K. S., C. P. Hu, and C. M. Chang.** 1991. Differential formation of disulfide linkages in the core antigen of extracellular and intracellular hepatitis B virus core particles. J. Virol. **65**:3924–3927.
22. **Kato, N., M. Hijikata, Y. Ootsuyama, M. Nakagawa, S. Ohkoshi, T. Sug-**

imura, and K. Shimotohno. 1990. Molecular cloning of the human hepatitis C virus genome from Japanese patients with non-A, non-B hepatitis. Proc. Natl. Acad. Sci. U. S. A. **87:**9524–9528.
23. **Kieffer, T. L., A. D. Kwong, and G. R. Picchio.** 2010. Viral resistance to specifically targeted antiviral therapies for hepatitis C (STAT-Cs). J. Antimicrob. Chemother. **65:**202–212.
24. **Kim, M., Y. Ha, and H. J. Park.** 2006. Structural requirements for assembly and homotypic interactions of the hepatitis C virus core protein. Virus Res. **122:**137–143.
25. **Koutsoudakis, G., A. Kaul, E. Steinmann, S. Kallis, V. Lohmann, T. Pietschmann, and R. Bartenschlager.** 2006. Characterization of the early steps of hepatitis C virus infection by using luciferase reporter viruses. J. Virol. **80:**5308–5320.
26. **Lee, J. Y., D. Hwang, and S. Gillam.** 1996. Dimerization of rubella virus capsid protein is not required for virus particle formation. Virology **216:**223–227.
27. **Li, M., P. Beard, P. A. Estes, M. K. Lyon, and R. L. Garcea.** 1998. Intercapsomeric disulfide bonds in papillomavirus assembly and disassembly. J. Virol. **72:**2160–2167.
28. **Li, P. P., A. Nakanishi, S. W. Clark, and H. Kasamatsu.** 2002. Formation of transitory intrachain and interchain disulfide bonds accompanies the folding and oligomerization of simian virus 40 Vp1 in the cytoplasm. Proc. Natl. Acad. Sci. U. S. A. **99:**1353–1358.
29. **Liang, T. J., L. J. Jeffers, K. R. Reddy, M. De Medina, I. T. Parker, H. Cheinquer, V. Idrovo, A. Rabassa, and E. R. Schiff.** 1993. Viral pathogenesis of hepatocellular carcinoma in the United States. Hepatology **18:**1326–1333.
30. **Liljas, L.** 1999. Virus assembly. Curr. Opin. Struct. Biol. **9:**129–134.
31. **Majeau, N., R. Fromentin, C. Savard, M. Duval, M. J. Tremblay, and D. Leclerc.** 2009. Palmitoylation of hepatitis C virus core protein is important for virion production. J. Biol. Chem. **284:**33915–33925.
32. **Matsumoto, M., S. B. Hwang, K. S. Jeng, N. Zhu, and M. M. Lai.** 1996. Homotypic interaction and multimerization of hepatitis C virus core protein. Virology **218:**43–51.
33. **McLauchlan, J.** 2000. Properties of the hepatitis C virus core protein: a structural protein that modulates cellular processes. J. Viral Hepat. **7:**2–14.
34. **McLauchlan, J., M. K. Lemberg, G. Hope, and B. Martoglio.** 2002. Intramembrane proteolysis promotes trafficking of hepatitis C virus core protein to lipid droplets. EMBO J. **21:**3980–3988.
35. **Menez, R., M. Bossus, B. H. Muller, G. Sibai, P. Dalbon, F. Ducancel, C. Jolivet-Reynaud, and E. A. Stura.** 2003. Crystal structure of a hydrophobic immunodominant antigenic site on hepatitis C virus core protein complexed to monoclonal antibody 19D9D6. J. Immunol. **170:**1917–1924.
36. **Miyanari, Y., K. Atsuzawa, N. Usuda, K. Watashi, T. Hishiki, M. Zayas, R. Bartenschlager, T. Wakita, M. Hijikata, and K. Shimotohno.** 2007. The lipid droplet is an important organelle for hepatitis C virus production. Nat. Cell Biol. **9:**1089–1097.
37. **Moradpour, D., C. Englert, T. Wakita, and J. R. Wands.** 1996. Characterization of cell lines allowing tightly regulated expression of hepatitis C virus core protein. Virology **222:**51–63.
38. **Moradpour, D., F. Penin, and C. M. Rice.** 2007. Replication of hepatitis C virus. Nat. Rev. Microbiol. **5:**453–463.
39. **Murray, C. L., C. T. Jones, J. Tassello, and C. M. Rice.** 2007. Alanine scanning of the hepatitis C virus core protein reveals numerous residues essential for production of infectious virus. J. Virol. **81:**10220–10231.
40. **Nolandt, O., V. Kern, H. Muller, E. Pfaff, L. Theilmann, R. Welker, and H. G. Krausslich.** 1997. Analysis of hepatitis C virus core protein interaction domains. J. Gen. Virol. **78**(Pt 6):1331–1340.
41. **Okamoto, K., Y. Mori, Y. Komoda, T. Okamoto, M. Okochi, M. Takeda, T. Suzuki, K. Moriishi, and Y. Matsuura.** 2008. Intramembrane processing by signal peptide peptidase regulates the membrane localization of hepatitis C virus core protein and viral propagation. J. Virol. **82:**8349–8361.
42. **Sabile, A., G. Perlemuter, F. Bono, K. Kohara, F. Demaugre, M. Kohara, Y. Matsuura, T. Miyamura, C. Brechot, and G. Barba.** 1999. Hepatitis C virus core protein binds to apolipoprotein AII and its secretion is modulated by fibrates. Hepatology **30:**1064–1076.
43. **Santolini, E., G. Migliaccio, and N. La Monica.** 1994. Biosynthesis and biochemical properties of the hepatitis C virus core protein. J. Virol. **68:**3631–3641.
44. **Seeff, L. B., and J. H. Hoofnagle.** 2003. Appendix: The National Institutes of Health Consensus Development Conference Management of Hepatitis C 2002. Clin. Liver Dis. **7:**261–287.
45. **Sekine-Osajima, Y., N. Sakamoto, K. Mishima, M. Nakagawa, Y. Itsui, M. Tasaka, Y. Nishimura-Sakurai, C. H. Chen, T. Kanai, K. Tsuchiya, T. Wakita, N. Enomoto, and M. Watanabe.** 2008. Development of plaque assays for hepatitis C virus-JFH1 strain and isolation of mutants with enhanced cytopathogenicity and replication capacity. Virology **371:**71–85.
46. **Senkevich, T. G., C. L. White, E. V. Koonin, and B. Moss.** 2000. A viral member of the ERV1/ALR protein family participates in a cytoplasmic pathway of disulfide bond formation. Proc. Natl. Acad. Sci. U. S. A. **97:**12068–12073.
47. **Shavinskaya, A., S. Boulant, F. Penin, J. McLauchlan, and R. Bartenschlager.** 2007. The lipid droplet binding domain of hepatitis C virus core protein is a major determinant for efficient virus assembly. J. Biol. Chem. **282:**37158–37169.
48. **Shimakami, T., R. E. Lanford, and S. M. Lemon.** 2009. Hepatitis C: recent successes and continuing challenges in the development of improved treatment modalities. Curr. Opin. Pharmacol. **9:**537–544.
49. **Tellinghuisen, T. L., M. J. Evans, T. von Hahn, S. You, and C. M. Rice.** 2007. Studying hepatitis C virus: making the best of a bad virus. J. Virol. **81:**8853–8867.
50. **Tellinghuisen, T. L., and C. M. Rice.** 2002. Interaction between hepatitis C virus proteins and host cell factors. Curr. Opin. Microbiol. **5:**419–427.
51. **Thompson, A. J., and J. G. McHutchison.** 2009. Antiviral resistance and specifically targeted therapy for HCV (STAT-C). J. Viral Hepat. **16:**377–387.
52. **Tscherne, D. M., C. T. Jones, M. J. Evans, B. D. Lindenbach, J. A. McKeating, and C. M. Rice.** 2006. Time- and temperature-dependent activation of hepatitis C virus for low-pH-triggered entry. J. Virol. **80:**1734–1741.
53. **Wakita, T., T. Pietschmann, T. Kato, T. Date, M. Miyamoto, Z. Zhao, K. Murthy, A. Habermann, H. G. Krausslich, M. Mizokami, R. Bartenschlager, and T. J. Liang.** 2005. Production of infectious hepatitis C virus in tissue culture from a cloned viral genome. Nat. Med. **11:**791–796.
54. **Wootton, S. K., and D. Yoo.** 2003. Homo-oligomerization of the porcine reproductive and respiratory syndrome virus nucleocapsid protein and the role of disulfide linkages. J. Virol. **77:**4546–4557.
55. **Zhou, S., and D. N. Standring.** 1992. Cys residues of the hepatitis B virus capsid protein are not essential for the assembly of viral core particles but can influence their stability. J. Virol. **66:**5393–5398.
56. **Zhou, S., and D. N. Standring.** 1992. Hepatitis B virus capsid particles are assembled from core-protein dimer precursors. Proc. Natl. Acad. Sci. U. S. A. **89:**10046–10050.
57. **Zweig, M., C. J. Heilman, Jr., and B. Hampar.** 1979. Identification of disulfide-linked protein complexes in the nucleocapsids of herpes simplex virus type 2. Virology **94:**442–450.

OPEN ACCESS Freely available online

PLoS one

Hepatitis C Virus Controls Interferon Production through PKR Activation

Noëlla Arnaud[1], Stéphanie Dabo[1], Patrick Maillard[1], Agata Budkowska[1], Katerina I. Kalliampakou[2], Penelope Mavromara[2], Dominique Garcin[3], Jacques Hugon[4], Anne Gatignol[5], Daisuke Akazawa[6], Takaji Wakita[6], Eliane F. Meurs[1]*

1 Institut Pasteur, Unité Hépacivirus et Immunité Innée, Paris, France, 2 Hellenic Pasteur Institute, Molecular Virology Laboratory, Athens, Greece, 3 University of Geneva School of Medicine, Geneva, Switzerland, 4 Institut du Fer à Moulin, Inserm UMRS 839, Paris, France, 5 Lady Davis Institute for Medical Research, Virus-Cell Interactions, McGill University, Montréal, Canada, 6 National Institute of Infectious Diseases, Department of Virology II, Tokyo, Japan

Abstract

Hepatitis C virus is a poor inducer of interferon (IFN), although its structured viral RNA can bind the RNA helicase RIG-I, and activate the IFN-induction pathway. Low IFN induction has been attributed to HCV NS3/4A protease-mediated cleavage of the mitochondria-adapter MAVS. Here, we have investigated the early events of IFN induction upon HCV infection, using the cell-cultured HCV JFH1 strain and the new HCV-permissive hepatoma-derived Huh7.25.CD81 cell subclone. These cells depend on ectopic expression of the RIG-I ubiquitinating enzyme TRIM25 to induce IFN through the RIG-I/MAVS pathway. We observed induction of IFN during the first 12 hrs of HCV infection, after which a decline occurred which was more abrupt at the protein than at the RNA level, revealing a novel HCV-mediated control of IFN induction at the level of translation. The cellular protein kinase PKR is an important regulator of translation, through the phosphorylation of its substrate the eIF2α initiation factor. A comparison of the expression of luciferase placed under the control of an eIF2α-dependent ($IRES^{EMCV}$) or independent ($IRES^{HCV}$) RNA showed a specific HCV-mediated inhibition of eIF2α-dependent translation. We demonstrated that HCV infection triggers the phosphorylation of both PKR and eIF2α at 12 and 15 hrs post-infection. PKR silencing, as well as treatment with PKR pharmacological inhibitors, restored IFN induction in JFH1-infected cells, at least until 18 hrs post-infection, at which time a decrease in IFN expression could be attributed to NS3/4A-mediated MAVS cleavage. Importantly, both PKR silencing and PKR inhibitors led to inhibition of HCV yields in cells that express functional RIG-I/MAVS. In conclusion, here we provide the first evidence that HCV uses PKR to restrain its ability to induce IFN through the RIG-I/MAVS pathway. This opens up new possibilities to assay PKR chemical inhibitors for their potential to boost innate immunity in HCV infection.

Citation: Arnaud N, Dabo S, Maillard P, Budkowska A, Kalliampakou KI, et al. (2010) Hepatitis C Virus Controls Interferon Production through PKR Activation. PLoS ONE 5(5): e10575. doi:10.1371/journal.pone.0010575

Editor: Sung Key Jang, Pohang University of Science and Technology, Republic of Korea

Received January 13, 2010; **Accepted** April 16, 2010; **Published** May 11, 2010

Funding: Financial support was provided by grants from Institut Pasteur (IP) and CNRS (URA3015). Noella Arnaud is recipient of Ministère de l'Education et de la Recherche fellowship. The funders had no role in study design, data collection and analysis, decision to publish, or preparation of the manuscript.

Competing Interests: The authors have declared that no competing interests exist.

* E-mail: emeurs@pasteur.fr

Introduction

In response to invasion with bacterial or viral pathogens, cells are able to mount an immediate immune response through their ability to use specialized cellular molecules, referred to as pattern recognition receptors or PRRs, to detect unusual DNA, ssRNA or dsRNA structures. Among these PRRs, are the CARD-containing DexD/H RNA helicases RIG-I and MDA5, which are activated upon binding either to both 5′-triphosphate ssRNA and short double-stranded RNA structures (RIG-I) or to long dsRNA and higher-ordered RNA structures (MDA5) [1]. Once activated, these RNA helicases interact with the mitochondria-bound MAVS adapter protein [2]. In the case of RIG-I, the interaction with MAVS requires ubiquitination of the CARD domain of RIG-I by the TRIM25 ubiquitin ligase [3]. Subsequently, MAVS is able to recruit the IKK complex and the TBK1/IKKε kinases that are responsible for the activation of the NF-κB and IRF3/IRF7 transcription factors, respectively. This leads to induction of the interferons and pro-inflammatory cytokines that are involved in the innate immune response [4].

Hepatitis C virus (HCV) (*Hepacivirus* genus within the *Flaviviridae* family) is one of the RIG-I-activating viruses [4], because of its 5′ppp-structured RNA, 3′-structured genomic RNA and replicative RNA duplexes [5]. In particular, its 3′-end poly-U/UC motif has been shown to function in conjunction with the 5′ppp as the HCV structure that activates RIG-I [6].

In contrast to other RIG-I activating viruses such as Sendai virus, influenza, or vesicular stomatitis virus [1], HCV is a poor inducer of IFN and pro-inflammatory cytokines in cell culture systems. One reason for this is that the HCV NS3/4A protease cleaves MAVS, resulting in a rapid disruption of the function of MAVS and in abrogation of the IFN induction pathway [2]. However, data presented in some studies performed using Huh7 hepatoma cells infected with cell-culture generated JFH1 virus showed that the IFN pathway was poorly activated even before full cleavage of MAVS, since only limited nuclear translocation of

IRF3 could be detected [7,8]. Similarly, in another study, infection of Huh7 cells with JFH1 did not lead to any IFN induction, whereas the cells responded well to transfection by synthetic dsRNA poly(I)-poly(C) [9]. Thus, the early events leading to IFN induction after RIG-I activation by HCV are still not well-characterized.

Here, we have re-addressed the question as to whether HCV infection can activate RIG-I/MAVS before cleavage of MAVS by the NS3/4A protease, by performing kinetics of infection with JFH1 in the newly described JFH1-permissive Huh7.25/CD81 cells, which were manipulated to present a functional RIG-I/MAVS pathway. Our results show that HCV infection can stimulate the IFN induction pathway up to 12 hrs post-infection, whereas detection of MAVS cleavage begins at 18 hrs post-infection and is maximal at 24 hrs. Importantly, our data reveal that 12 hrs post-infection, HCV promotes a rapid inhibition of IFN induction at the level of translation, indicating a new mechanism of regulation. We demonstrated that this regulation was linked to activation of the dsRNA-activated eIF2α kinase PKR [10]. Altogether, our results show that HCV uses PKR to control the translation of newly transcribed IFN mRNAs before sufficient NS3/4A protein can be synthesized to efficiently restrain transcription of IFN.

Results

Ectopic expression of TRIM25 allows IFN induction in JFH1 permissive Huh7.25/CD81 cells to be studied

There is at present no satisfactory cell culture system that is both permissive for HCV and presents an intact RIG-I pathway. For instance, the Huh7.5 cells, which were cloned from the hepatoma Huh7 cells for their efficacy to support HCV replication [11], are unable to stimulate IFN induction because of a T55I substitution in the first CARD domain of RIG-I that prevents the association of RIG-I with MAVS [5]. Recently, another Huh7 subclone that could efficiently replicate the JFH1 subgenomic replicon (clone Huh7.25) was stably transfected with the essential HCV CD81 receptor, to generate Huh7.25/CD81 cells that are highly permissive to infection by JFH1[12]. We compared the ability of Huh7.25/CD81, Huh7.5 and Huh7 cells to activate the IFN inducing pathway after transfection with an IFNβ-luciferase reporter and infection with Sendai virus (Figure 1). The results showed that Huh7.25/CD81 cells are defective in the IFN-inducing pathway, similarly to Huh7.5 cells. In contrast, Huh7 cells can mount a robust IFN induction in response to infection with Sendai virus. Interestingly, whereas ectopic expression of MAVS in both Huh7.25/CD81 and Huh7.5 cells resulted in a strong stimulation of IFNβ-luciferase, ectopic expression of RIG-I was not able to restore the IFN-inducing pathway in Huh7.25/CD81 cells, in contrast to in Huh7.5 cells where it was able to do so as expected. This indicated that the defect in Huh7.25/CD81 cells was upstream of MAVS and either at the level of RIG-I or downstream of RIG-I. Since efficient activation of MAVS by RIG-I has been shown to depend upon the ubiquitination of RIG-I by the ubiquitin ligase TRIM25 [3], we assayed the effect of TRIM25 in Huh7.25/CD81 cells. Ectopic expression of TRIM25 in Huh7.25/CD81 cells had no effect alone, but resulted in a strong induction of IFN when the cells were infected with Sendai virus, indicating that these cells present a defect in the RIG-I/MAVS pathway at the level of TRIM25. Whatever the nature of this

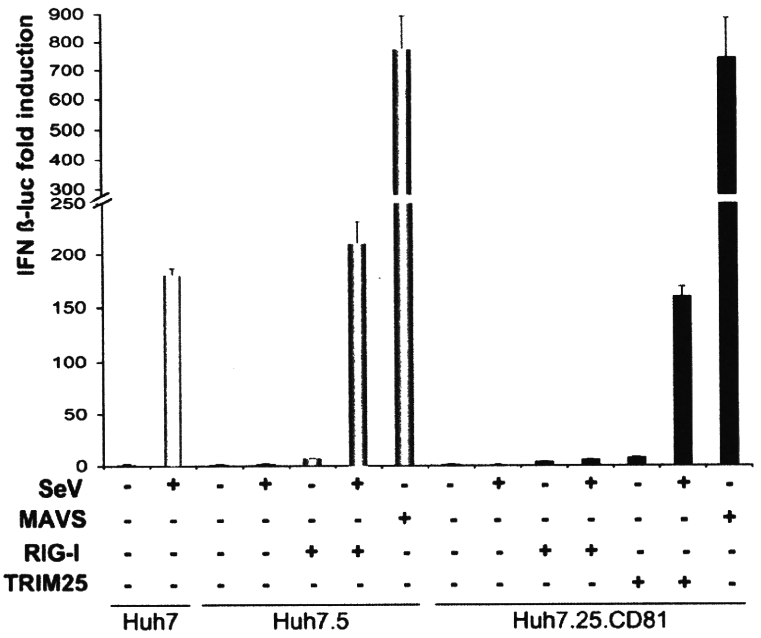

Figure 1. Ectopic expression of TRIM25 restores IFN induction in Huh7.25.CD81 cells. Huh7, Huh7.5 and Huh7.25.CD81 cells were transfected with the pGL2-IFNβ-FLUC/pRL-TK-RLUC reporter plasmids alone or the in presence of plasmids expressing RIG-I (200 ng), TRIM25 (100 ng) or MAVS (400 ng). 24 hrs post transfection, cells were mock-infected or infected with Sendaï virus (SeV) (40 HAU/ml). 24 hrs after infection, luciferase activity was measured and F-luc was normalized against R-luc. IFN expression was expressed as fold induction over control cells that were simply transfected with pGL2-IFNβ-FLUC/pRL-TK-RLUC. Error bars represent the mean ± S.D. for triplicates.
doi:10.1371/journal.pone.0010575.g001

defect, ectopic expression of TRIM25 now allows the use of Huh7.25/CD81 cells as a model to examine the effect of HCV infection on the IFN induction pathway.

HCV specifically stimulates the IFN induction pathway during the first 12 hrs of infection, but inhibits it thereafter

To estimate the time-frame required to study IFN induction before its abrogation upon the action of NS3/4A, we first established the kinetics of MAVS cleavage in the two HCV permissive cell lines Huh7.25/CD81 and Huh7.5 following HCV infection. MAVS cleavage can be detected by immunoblotting, which shows a progressive diminution of the MAVS full-length protein (540 aa) and the apparition of a MAVS cleavage product (513 aa) [2]. In our experimental conditions, MAVS cleavage was clearly detected in both cell types at 48 hrs after infection with JFH1 (Figures 2A and B). Since ectopic expression of TRIM25 in Huh7.25/CD81 cells will be needed in our subsequent experiments designed to examine the effects of HCV on the IFN induction pathway, we also established the kinetics of MAVS cleavage in these cells after their transfection with a plasmid that expresses HA-TRIM25. Under these conditions, MAVS cleavage was clearly observed at 48 hrs (Figure 2C). In all cases, the viral NS3 protease was detected as early as 18–24 hrs, and thereafter its expression increased strongly with time, concomitantly with MAVS cleavage.

Huh7.25/CD81 or Huh7.5 cells were transfected with an IFNβ-luciferase reporter plasmid in the presence of limited amounts of TRIM25 or RIG-I, respectively, and infected with HCV at an moi of 0.2 or with Sendai virus as control. In case of HCV infection, analysis of luciferase activity or of the expression of endogenous IFNβ RNA and HCV RNA was performed in parallel. The results show an increase in luciferase activity that corresponds to an increase in the activation of the RIG/MAVS pathway (Figure 3A,C bottom). This increase was detected as early as 6 hrs after infection for Huh7.25/CD81 cells and 10.5 hrs for Huh7.5 cells, with a maximum expression at 12 hrs for both cell types. The data of the reporter assay were also confirmed at the endogenous level when induction of endogenous IFNβ RNA was assessed by RTqPCR (Figure 3B,D). In both cases, the expression

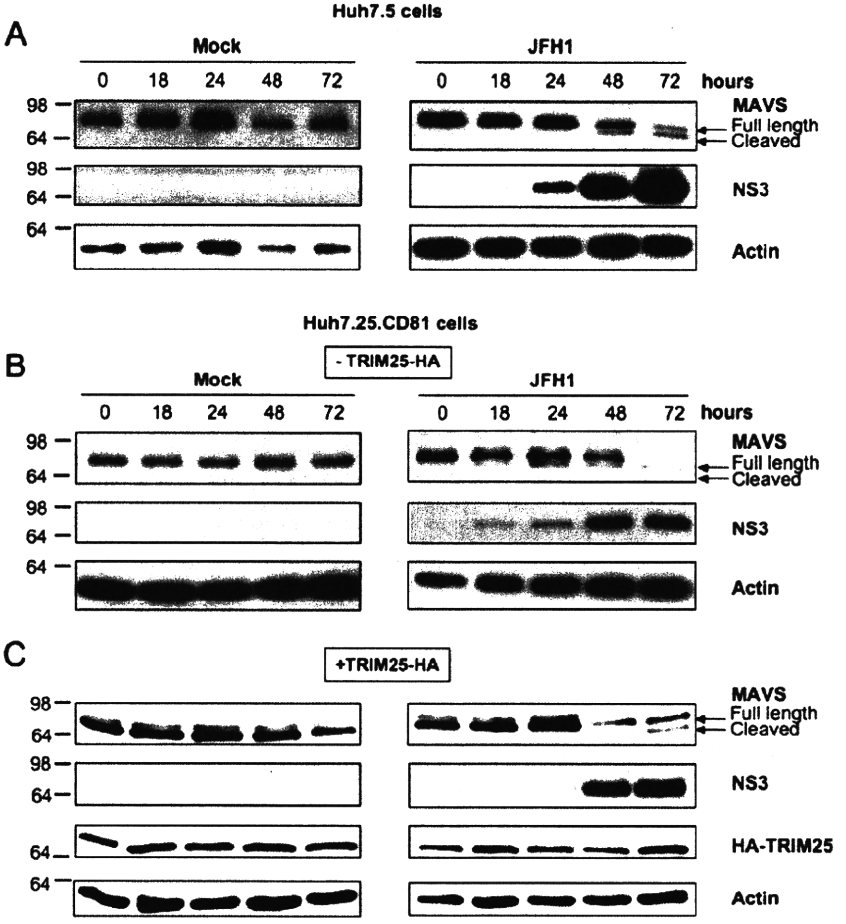

Figure 2. Kinetics of MAVS cleavage in Huh7.25.CD81 cells after JFH1 infection. Huh7.5 cells and Huh7.25.CD81 cells were transfected with an HA-TRIM25 expressing plasmid or with an empty plasmid. 24 hrs post-transfection, cells were mock-infected or infected with JFH1 (m.o.i = 0.05) for the indicated times and cell lysates were generated. Cell extracts (50 μg) were subjected to SDS-12.5% PAGE and blotted with anti-MAVS, anti-NS3, anti-HA or anti-actin as indicated. The arrows indicate the position of full-length MAVS and MAVS cleaved in the presence of HCV NS3/4A.
doi:10.1371/journal.pone.0010575.g002

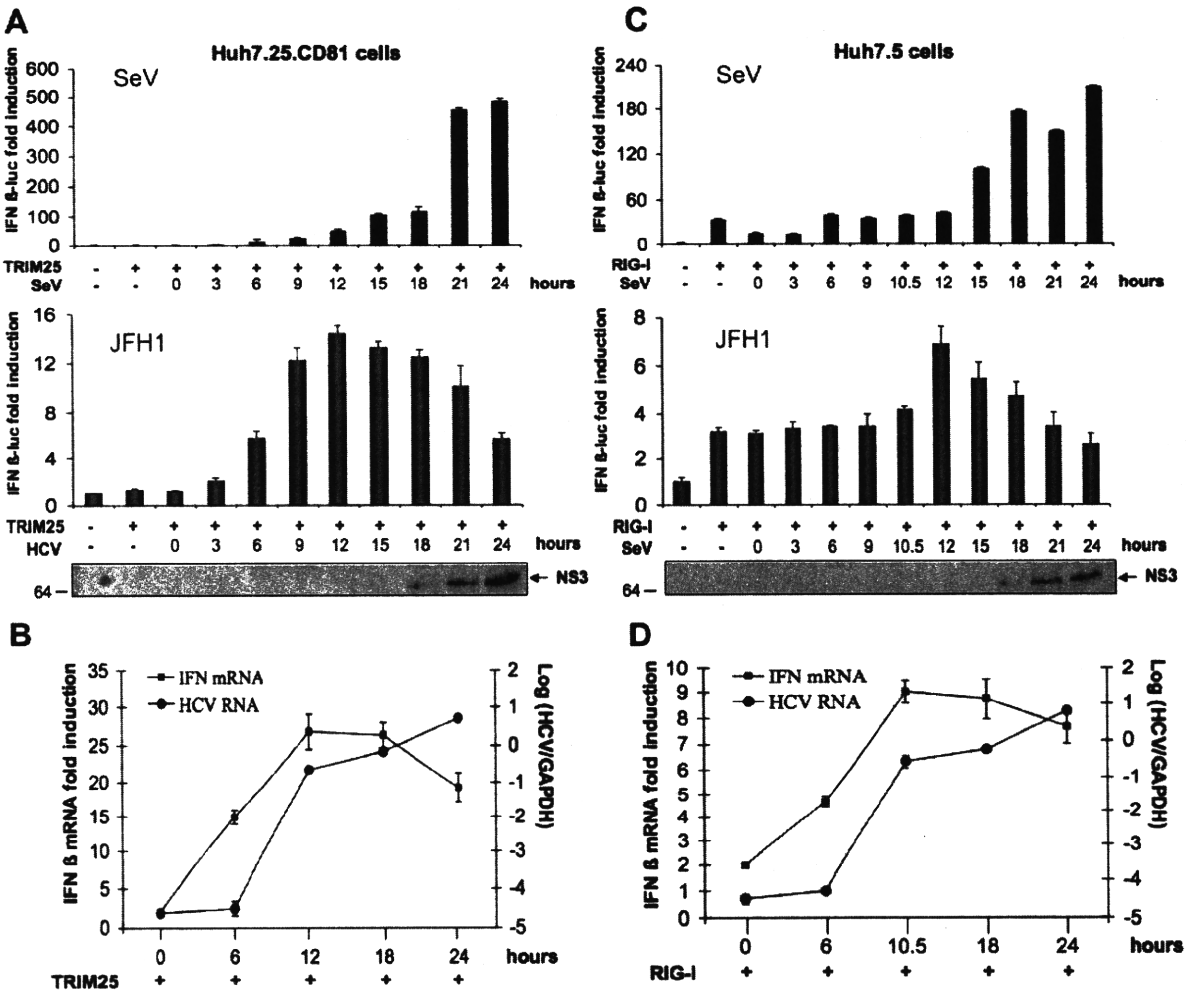

Figure 3. HCV induces IFN during the first 12 hrs of infection and inhibits it thereafter. Huh7.25.CD81 and Huh7.5 cells were transfected with the pGL2-IFNβ-FLUC/pRL-TK-RLUC reporter plasmids together with plasmids expressing HA-TRIM25 (Huh7.25.CD81; A and B) or RIG-I (Huh7.5; C and D). 24 h post-transfection, the cells were infected with SeV (40 HAU/ml) or JFH1 (m.o.i = 0.2). **A and C**: 24 hrs post-transfection, the cells were infected with SeV (40 HAU/ml) or JFH1 (m.o.i = 0.2). At the times indicated, cell lysates were prepared and analysed for IFN induction as described in Materials and Methods. The graphs represent the levels of F-luc activity normalized to R-luc RNA expressed as IFN-β fold-induction over control cells that were simply transfected with pGL2-IFNβ-FLUC/pRL-TK-RLUC. Error bars represent the mean ± S.D. for triplicates. In addition, cell lysates from JFH1-infected cells were pooled and analysed for the presence of NS3 as a marker of HCV infection. **B and D**: 24 hrs post-transfection, Huh7.25.CD81 and Huh7.5 cells were infected with JFH1 (m.o.i = 0.2). At the times indicated, cells were processed for RNA extraction and HCV or IFNβ RNA were quantified by qRT-PCR respectively, and normalized against RNA from GAPDH. Error bars represent the mean ± S.D. for triplicates.
doi:10.1371/journal.pone.0010575.g003

of the viral HCV RNA increases from 6 hrs after infection and continues to rise thereafter. These results indicate that HCV can activate the RIG-I signalling pathway with concomitant IFN induction within the first 12 hrs of infection.

Intriguingly, we observed that after 12 hrs of infection, there was a considerable decline of luciferase activity in both cell types, whereas the levels of endogenous IFNβ RNA remained at a plateau level until 18 hrs, before decreasing at 24 hrs post-infection. The decrease in luciferase expression between 12 and 18 hrs was surprising since NS3 was not fully expressed within this period of time (Figure 3A,C). In contrast, a decrease in luciferase expression at 24 hrs was expected, due to the massive proteolytic cleavage of MAVS by the HCV NS3/4A protease (Figure 2). Inhibition of luciferase activity was shown to be specific to HCV, as infection of both cell types with Sendai virus resulted in a continuous increase of luciferase activity from the IFNβ-luc reporter plasmid (Figure 3A,C top). Altogether, our data indicate that HCV can activate the IFN induction pathway within 12 hrs after infection, but blocks it prior to the NS3/4A-mediated cleavage of MAVS.

HCV activates the phosphorylation of PKR and of its substrate eIF2α, as of 12 hrs post-infection

The results shown in Figure 3 suggested a control of IFN expression by HCV at the protein level. In addition to this, an analysis of the effect of infection on the activity of a different luciferase reporter construct (TK-Renilla luciferase; Figure S1)

revealed a similar specific inhibition at 12 hrs post-infection with HCV and not with Sendaï virus, indicating that HCV could exert a control on protein expression at the general translational level. One possible candidate that could exert such a control is the protein kinase PKR, which inhibits protein synthesis through phosphorylation of the initiation factor eIF2α [13]. Activation of the catalytic domain of PKR is mediated by a change in its conformation due to the interaction of its N terminus with dsRNA structures or with specific proteins [10]. The fact that IFN could be induced during the first 12 hrs post-infection with JFH1 in Huh7.25.CD81/TRIM25 or in Huh7.5/RIG-I cells was an indication that HCV dsRNA structures had appeared in the cytosol that activate RIG-I and that these structures may also represent good candidates to activate PKR. We therefore examined the state and dynamics of phosphorylation of PKR and of its substrate eIF2α upon HCV infection, using Huh7.25/CD81 cells, either as such or upon ectopic expression of TRIM25. At different times post-infection, cell extracts were immunoprecipitated with antibodies directed against PKR or eIF2α, after which the degree of PKR or eIF2α phosphorylation was examined using anti-phospho PKR (residue Thr451) or anti-phospho eIF2α (residue Ser51) antibodies and by performing quantification of the p-PKR/PKR or the p-eIF2α/eIF2α ratio. The results clearly showed peaks of PKR (Figure 4) and eIF2α (Figure 5) phosphorylation as early as 12 and 15 hrs post-infection, followed by a decrease of phosphorylation until 24 hrs and a second increase until 72 hrs post-infection, the end-point of the experiment. The presence of TRIM25 was not found to significantly affect PKR or eIF2α phosphorylation, except for a less abrupt decline between15 and 24 hrs. Altogether, these results show that PKR and its substrate eIF2α are activated in the early hours of HCV infection.

HCV infection triggers inhibition of protein translation

HCV belongs to the family of viruses with 5′ IRES structures that are translated after direct binding of ribosomes to the RNA in the vicinity of the initiation codon. Interestingly, unlike most viral

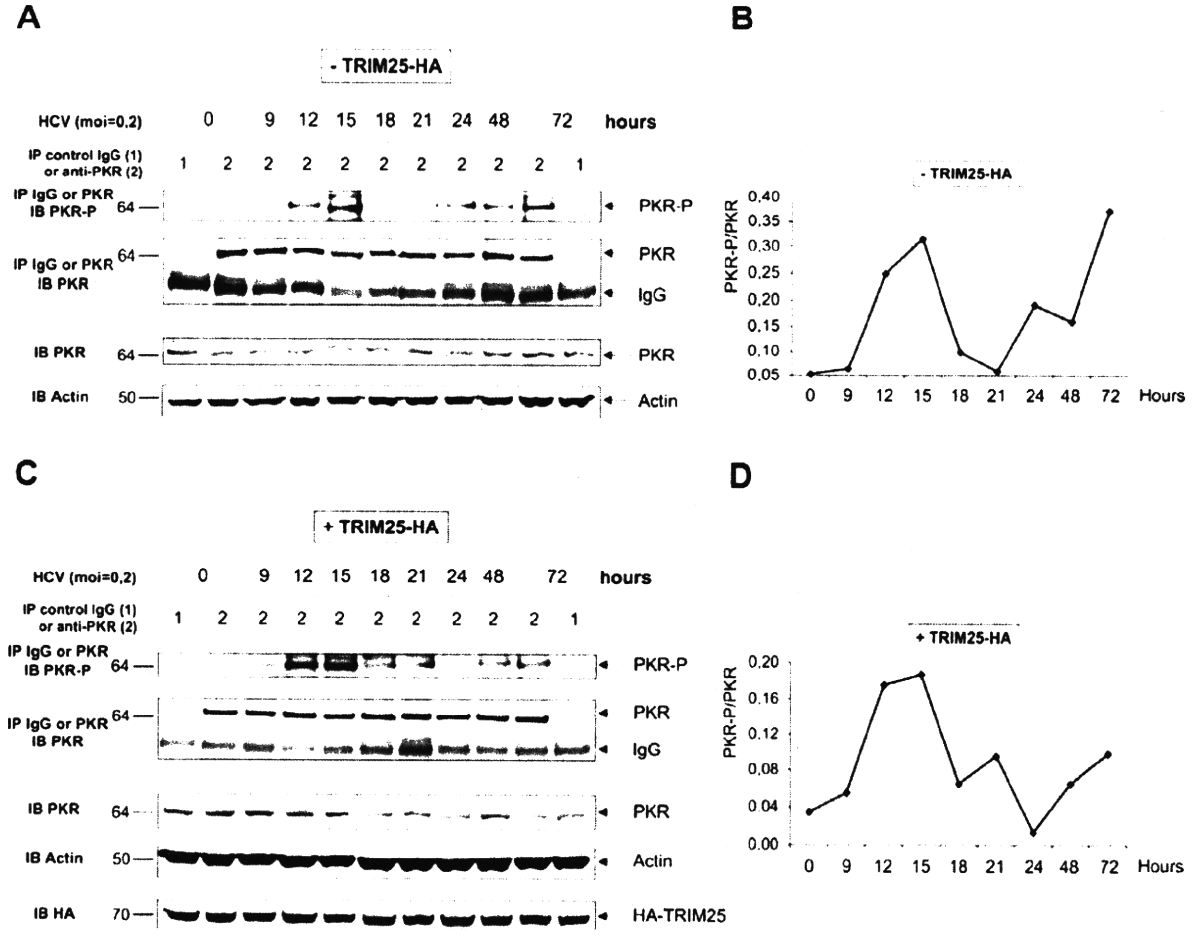

Figure 4. HCV activates the phosphorylation of PKR at 12 and 15 hrs post infection. A and C: Huh7.25.CD81 cells, plated into 100 cm^2 plates, were transfected with the HA-TRIM25 expressing plasmid or with an empty plasmid. 24 hrs post-transfection, cells were infected with JFH1 at an m.o.i of 0.2. At the indicated times post-infection, cell extracts (1 mg) were incubated with Mab 71/10 anti-PKR. In addition, cell extracts prepared at time 0 or at 72 hrs p.i. were incubated with mouse IgG as a control of specificity. The immunoprecipitated complexes were run on two different NuPAGE gels and blotted using Mab 71/10 or anti-phosphorylated PKR (PKR-P). The presence of PKR and PKR-P was revealed using the Odyssey procedure. **B and D**: The bands corresponding to total PKR and their corresponding phosphorylated proteins were quantified using the Odyssey software and expressed as the ratio PKR-P/PKR in the absence (B) or presence (D) of HA-TRIM25.
doi:10.1371/journal.pone.0010575.g004

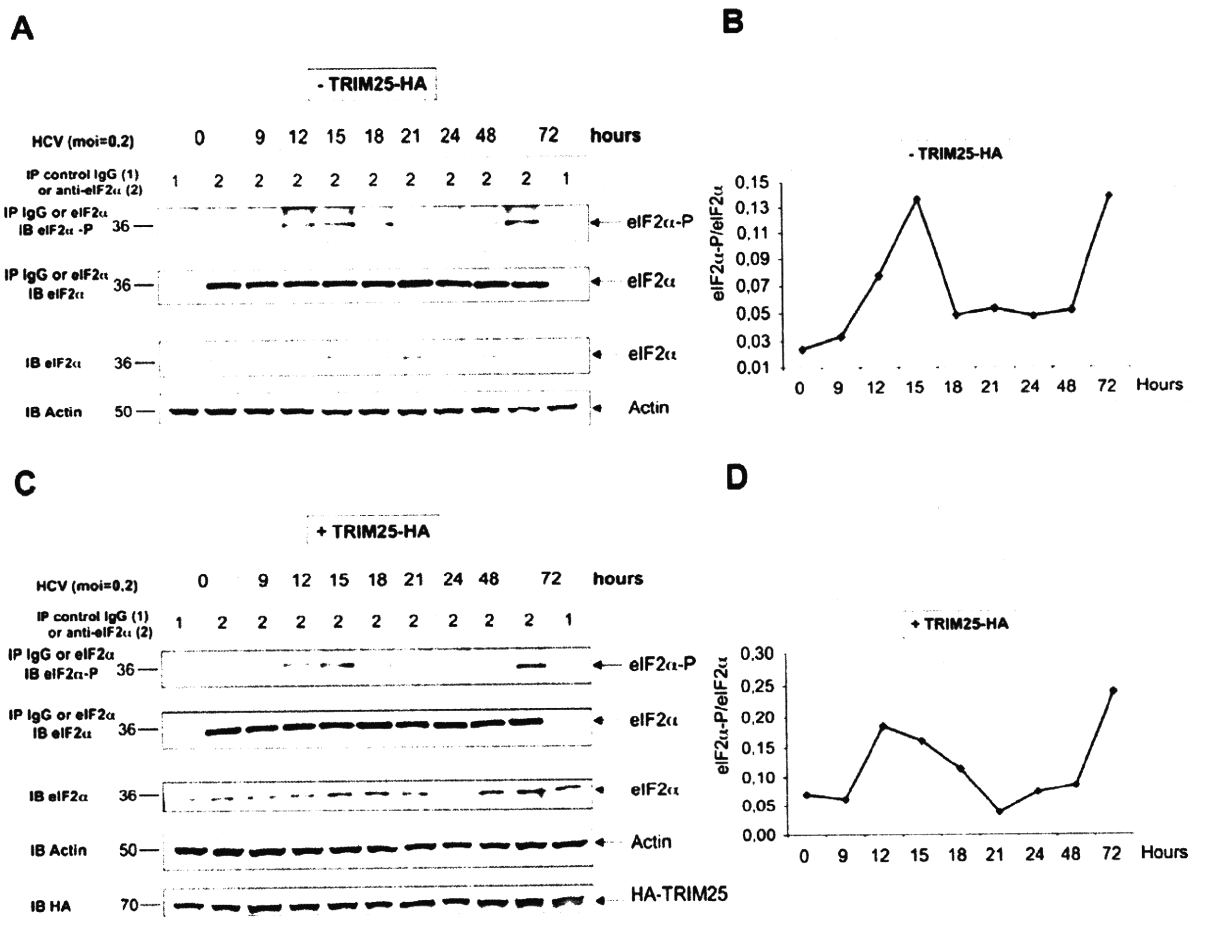

Figure 5. HCV activates the phosphorylation of eIF2α at 12 and 15 hrs post infection. The detection of eIF2α and eIF2α-P and the quantification of the ratio eIF2α-P/eIF2α in the absence (**A and B**) or in the presence (**C and D**) of HA-TRIM25 was performed as described in the legend to Figure 4.

doi:10.1371/journal.pone.0010575.g005

IRESs, translation from the HCV IRES was shown to be independent of eIF2α phosphorylation in situations of stress [14,15]. To establish a correlation between the observed HCV-mediated PKR and eIF2α phosphorylation, and a possible inhibition of eIF2α-dependent translation by HCV, we next compared the effects of HCV infection on the kinetics of expression of a luciferase reporter placed under the control of the IRES^{HCV} (insensitive to eIF2α phosphorylation) or under that of the IRES ^{EMCV} (sensitive to eIF2α phosphorylation). The experiment was done in Huh7.25/CD81 cells transfected with a TRIM25-expressing plasmid, to perform the analysis in conditions leading to IFN induction. For each IRES-luc expressing plasmid, we took care to choose concentrations of these plasmids that give similar levels of RNA expression or luciferase activity (data not shown and Figure 6). After transfection by the different plasmids, the cells were infected with JFH1 and the levels of RNA or luciferase expression followed over 24 hrs. The expression levels of IRES ^{EMCV} RNA and IRES ^{HCV} RNA were found to increase similarly with time post-infection (Figures 6A and C). In contrast, there was a dramatic difference in the expression levels of luciferase expressed from the IRES ^{EMCV} compared to that expressed from the IRES ^{HCV} (Figures 6B and D). Expression of luciferase from the IRES ^{EMCV} was strongly inhibited at 12 hrs post-infection with JFH1, after which time it was progressively restored until at 24 hrs post-infection it approached its initial level. In contrast, expression of luciferase from the HCV IRES was not inhibited at any time after infection with JFH1. Rather, it steadily increased with time post-infection. Similarly to the experiment presented in Figure 3, concomitant analysis of luciferase activity placed under a TK promoter revealed inhibition at 12 hrs post-infection with HCV, regardless of the presence of IRES ^{EMCV} or IRES ^{HCV}, again indicating that the inhibition effect is due to HCV infection and occurs at a general level (Figure S2). These results demonstrate that HCV infection triggers inhibition of general translation, while translation from the IRES ^{HCV} is unaffected. Since inhibition of translation occurs at 12 hrs post-infection, at a time when PKR and eIF2α are phosphorylated (Figures 4 and 5), this shows a correlation between an HCV-mediated inhibition of protein synthesis and PKR/eIF2α phosphorylation; a hallmark of eIF2α-dependent translation.

Depletion of PKR increases IFN induction

We next examined further the role of the ability of HCV to activate PKR in the early events of infection, in relation to IFN